UNCLASSIFIED

~~RESTRICTED~~

~~CONFIDENTIAL~~

COPY NO. 6

RM No. E8B19

Copy

29 SEP 1948

CLASSIFICATION CHANGED

To ~~RESTRICTED~~

NACA

NACA Release form #636,

By authority of H. L. Dryden Date July 3, 1951

by HLR 7-13-51

RESEARCH MEMORANDUM

ALTITUDE-WIND-TUNNEL INVESTIGATION OF A 3000-POUND-THRUST AXIAL-FLOW TURBOJET ENGINE

III - ANALYSIS OF COMBUSTION-CHAMBER PERFORMANCE

By Carl E. Campbell

Flight Propulsion Research Laboratory
Cleveland, Ohio

CLASSIFICATION CANCELLED

Authority J. W. Crowley Date 12/8/53

GEO 10561

By MHA 12/22/53 See NACA

RF 1700

SPECIAL RELEASE

TRANSMITTED ON

NOT TO BE INDEXED, REFERENCED, OR GIVEN FURTHER DISTRIBUTION WITHOUT APPROVAL OF NACA.

CLASSIFIED DOCUMENT

This document contains classified information affecting the National Defense of the United States within the meaning of the Espionage Act, USC 50:31 and 32. Its transmission or the revelation of its contents in any manner to an unauthorized person is prohibited by law. Information so classified may be imparted only to persons in the military and naval services of the United States, appropriate civilian officers and employees of the Federal Government who have a legitimate interest therein, and to United States citizens of known loyalty and discretion who of necessity must be informed thereof.

TECHNICAL EDITING WAIVED

NATIONAL ADVISORY COMMITTEE FOR AERONAUTICS

WASHINGTON
August 23, 1948

~~CONFIDENTIAL~~

NACA LIBRARY
LANGLEY MEMORIAL AERONAUTICAL LABORATORY
Langley Field, Va.

UNCLASSIFIED

~~RESTRICTED~~

NASA Technical Library
3 1176 01435 5060

~~RESTRICTED~~ UNCLASSIFIED

NATIONAL ADVISORY COMMITTEE FOR AERONAUTICS

RESEARCH MEMORANDUM

ALTITUDE-WIND-TUNNEL INVESTIGATION OF A 3000-POUND-THRUST AXIAL-FLOW TURBOJET ENGINE

III - ANALYSIS OF COMBUSTION-CHAMBER PERFORMANCE

By Carl E. Campbell

SUMMARY

Combustion-chamber performance characteristics of a 3000-pound-thrust axial-flow turbojet engine have been determined from an investigation of the complete engine in the NACA Cleveland altitude wind tunnel. Data are presented for a range of simulated altitudes from 15,000 to 45,000 feet and a range of simulated flight Mach numbers from 0.23 to 1.05 for various modifications of the engine. The combustion-chamber performance characteristics are presented as functions of the engine speed corrected to NACA standard altitude inlet conditions. The effect of variations in altitude and flight Mach number on combustion efficiency, combustion-chamber total-pressure losses, engine-cycle efficiency, and the fractional loss in engine-cycle efficiency resulting from combustion-chamber pressure losses is presented for various engine configurations.

Combustion efficiency varied directly with engine speed and inversely with altitude, flight Mach number, and exhaust-nozzle-outlet area. Combustion-chamber pressure-loss ratios varied directly with flight Mach number and exhaust-nozzle-outlet area and inversely with altitude. Maximum total-pressure-loss ratios occurred at low or medium engine speeds. Lower percentage losses in combustion-chamber total pressure were obtained with the modified engine than with the other configurations. Engine-cycle efficiency varied directly with engine speed and altitude and inversely with exhaust-nozzle-outlet area. At high engine speeds, the engine-cycle efficiency varied directly with flight Mach number. The engine-cycle efficiency of the modified engine was considerably higher than that obtained with the original engine. The fractional losses in engine-cycle efficiency due to combustion-chamber pressure losses varied directly with flight Mach number at low engine speeds and inversely with engine speed and altitude. Engine operation with large exhaust-nozzle-outlet areas resulted in very high fractional losses in cycle efficiency.

UNCLASSIFIED

INTRODUCTION

An investigation to determine the performance and operational characteristics of an axial-flow turbojet engine having a thrust rating of 3000 pounds has been conducted in the NACA Cleveland altitude wind tunnel. The performance characteristics of the component parts of the turbojet engine were determined in addition to the evaluation of the over-all characteristics. The performance characteristics of the compressor and the turbine as determined from the investigation of the complete engine are presented in references 1 and 2, respectively.

An analysis of the performance of the combustion chamber with various modifications of the combustion basket, combustion-chamber-inlet screens, and fuel nozzles is presented herein. These modifications were made in an attempt to improve the turbine-inlet temperature distribution and the engine operating range at high altitude. The combustion efficiency, the engine-cycle efficiency, the losses in total pressure occurring in the combustion chamber, and the fractional loss in engine-cycle efficiency resulting from combustion-chamber pressure losses are compared for various engine configurations. Data for which performance characteristics are presented were obtained over a wide range of simulated altitudes and flight Mach numbers.

ENGINE AND INSTALLATION

The X24C-4B engine used in this investigation (fig. 1) has a static sea-level rating of 3000 pounds thrust at an engine speed of 12,500 rpm. At this rating the air flow is approximately 58.5 pounds per second, the fuel consumption is 3200 pounds per hour, and the compressor pressure ratio is 3.8. The main components of the engine include an 11-stage axial-flow compressor, a double-annulus combustion chamber, a two-stage turbine, and a fixed-area exhaust nozzle.

The main components of the original and modified engines used in the investigation were similar except for changes made by the manufacturer to the compressor (reference 1) and the combustion chamber. As a result of these modifications, the turbine-outlet temperature distribution was so improved (fig. 2) that the limiting turbine-outlet temperature was raised from 1710° to 1860° R as read on the hottest thermocouple. The flat temperature profile at the turbine outlet of the original engine resulted in critical temperatures near the root of the turbine blade. The nonuniform turbine-outlet temperature profile obtained with the modified engine

approached critical temperatures near the midpoint of the turbine blade, where the allowable temperature was much higher than near the blade root. A higher average turbine-outlet temperature was thereby permitted for the modified engine than for the original engine. The engine modifications and the resulting higher temperature limit at the turbine outlet permitted a reduction of the standard exhaust-nozzle area from 183 square inches for the original engine to 171 square inches for the modified engine.

925

The engine was mounted in a wing nacelle, which was installed in the 20-foot-diameter test section of the altitude wind tunnel (fig. 1). Inlet pressures corresponding to high flight Mach numbers were obtained by introducing dry refrigerated air from the tunnel make-up air system through a duct to the engine inlet. This air was throttled from approximately sea-level pressure to the desired pressure at the compressor inlet while the tunnel pressure corresponding to the desired altitude was maintained. The make-up air duct was connected to the engine intake duct by means of a slip joint with a labyrinth seal.

The stations at which instrumentation was installed are shown in figure 3. This report is mainly concerned with the combustion-chamber inlet or compressor outlet (station 4), the combustion-chamber outlet or turbine inlet (station 5), the turbine outlet (station 7), and the exhaust-nozzle outlet (station 8). Instrumentation at these stations is shown in detail in figures 4 to 8.

DESCRIPTION OF COMBUSTION CHAMBER

A cross-sectional drawing of the combustion chamber of the turbojet engine is shown in figure 3. The combustion zone is separated from the rest of the combustion section by a double-annulus basket that merges into a single annulus near the downstream end of the combustion chamber (fig. 9). The combined cross-sectional area of the combustion zones varies from approximately 1.73 square feet at the upstream end to about 2.67 square feet where the two annuli merge. A single row of holes on all four surfaces of each of the first two steps admits primary air to the combustion zones. A large number of "anticoking" holes on the upstream faces of the annuli and on the first-step surfaces admit air for retarding the deposition of carbon around the fuel nozzles. Secondary air enters the combustion zones of the original basket through four rows of circular holes in each surface of the third step and three rows of larger-diameter holes in the fourth-step surfaces. The basket used on the modified engine differed from the basket of the original

engine in that the holes on each surface of the fourth step were eliminated and the third step contained large rectangular holes with slightly rounded corners (fig. 10). The total area of the rectangular holes equaled the total area of the circular holes on both third and fourth steps of the original basket.

925

Combustion-chamber-inlet screens were installed in the plane adjacent to the upstream face of the basket in order to improve the air-flow distribution at the combustion-chamber inlet (fig. 11). On the original combustion chamber, the screen in the outer passage blocked 60 percent of the area and in the intermediate passage blocked 40 percent of the area. On the modified combustion chamber, the screens in both outer and intermediate passages blocked 30 percent of the area. In both combustion chambers, screens were omitted from the inner passage.

The original and modified combustion chambers were equipped with 60 fuel nozzles that have a rating of 7 gallons per hour at a differential pressure of 100 pounds per square inch and were mounted on two concentric manifold rings. These nozzles have a spray-cone angle of 80°. Thirty-six of these nozzles extended into the combustion zone at the upstream face of the outer-basket annulus and were equally spaced around the circumference. The inner manifold ring contained 24 fuel nozzles, which penetrated the combustion zone of the inner-basket annulus at even intervals. Sheet-metal fairings completely separated the fuel nozzles and manifold rings from the air flow between the compressor and the combustion chamber. Ignition was provided by two spark plugs that entered the bottom of the outer casing at angles of 45° with the vertical center line near the upstream end of the combustion chamber.

For one part of the investigation, the holes in the third step of the original combustion-chamber basket were blocked (fig. 12) in an attempt to improve the turbine-inlet temperature distribution. Fuel nozzles with ratings of $7\frac{1}{2}$ and 3 gallons per hour were used in addition to the 7-gallon-per-hour nozzles in an attempt to improve the operational characteristics of the engine at high altitude. The spray-cone angles of the $7\frac{1}{2}$- and 3-gallon-per-hour nozzles were 80° and 90°, respectively. With these nozzles installed on the engine, runs were conducted with all nozzles in operation and also with alternate nozzles blocked.

The various combustion-chamber modifications that were investigated are summarized in the following table:

Engine	Combustion-chamber basket	Blocking area of combustion-chamber-inlet screens (percent)	Fuel-nozzle capacity (gal/hr)	Number of fuel nozzles
Original	Original	60 and 40	7	60
Original	Original	60 and 40	$7\frac{1}{2}$	60
Original	Original	60 and 40	$7\frac{1}{2}$	30
Original	Original	60 and 40	3	60
Original	Original	60 and 40	3	30
Original	Third-step holes blocked	60 and 40	$7\frac{1}{2}$	60
Modified	Modified	30 and 30	7	60

PROCEDURE

Data are presented for a range of simulated altitudes from 15,000 to 45,000 feet, simulated flight Mach numbers from 0.23 to 1.05, and engine speeds from 4000 to 12,500 rpm. At high altitudes, the maximum engine speed was limited by high turbine-outlet temperatures and the minimum engine speed was limited by combustion blowout. The compressor-inlet-air temperature was maintained at approximately NACA standard temperature for each simulated flight condition except that no temperatures below -20° F, which correspond to high altitudes and low flight Mach numbers, were obtained. Four exhaust nozzles with outlet areas of 171, 189, 231, and 330 square inches were installed on the modified engine.

Air-flow calculations were made from pressure and temperature measurements obtained at the cowl inlet (station 1). The fuel flow was measured with a rotameter. The engine speeds were corrected to standard NACA temperatures corresponding to the simulated flight conditions.

RESULTS AND DISCUSSION

Engine speeds were not corrected to standard sea-level conditions, as customary with combustion-chamber data, because none of the data generalized. It was therefore believed that the true altitude effect would be more apparent if the data were presented in the ungeneralized form.

Combustion Efficiency

The variation of combustion efficiency with engine speed for the modified engine is shown in figure 13 for a range of simulated altitudes from 15,000 to 45,000 feet and flight Mach numbers of 0.71 and 0.52. Combustion efficiency increased rapidly with engine speed up to about 11,000 rpm. The maximum combustion efficiencies obtained at these altitudes and flight Mach numbers varied from 0.95 to 0.99 and occurred at the maximum engine speeds obtainable. In general, the combustion efficiency decreased with increased altitude at low engine speeds. All efficiencies obtained at 45,000 feet are of questionable accuracy because burning through the turbine may have occurred at this altitude and affected the temperatures at the turbine outlet.

The effect of flight Mach number on the combustion efficiency of the modified engine at simulated altitudes of 45,000 and 25,000 feet is shown in figure 14. Combustion efficiency decreased with an increase in flight Mach number at constant engine speed, particularly in the low engine-speed range. At engine speeds greater than 11,500 rpm at an altitude of 25,000 feet, the combustion efficiencies varied from 0.95 to 0.99 for a range of flight Mach numbers from 0.52 to 1.05 (fig. 14(b)).

The effect of exhaust-nozzle-outlet area on combustion efficiency is shown in figure 15. In general, combustion efficiency decreased when the exhaust-nozzle-outlet area was increased. The combustion efficiency obtained with the 189-square-inch nozzle, however, fell below the efficiencies obtained with larger exhaust-nozzle-outlet areas at high engine speeds.

Variation of combustion efficiency with engine speed for the various engine modifications at an altitude of 35,000 feet and a flight Mach number of 0.52 is shown in figure 16. Considerably higher combustion efficiencies were obtained with the 3-gallon-per-hour fuel nozzles than with any other configuration at this altitude, which is attributed to improved fuel atomization. The maximum efficiency obtained with these nozzles was 0.98 at 10,750 rpm, but the efficiency dropped off rapidly at higher engine speeds. Blocking one-half of the fuel nozzles had very little effect on combustion efficiency. The $7\frac{1}{2}$-gallon-per-hour fuel nozzles gave higher efficiencies than the 7-gallon-per-hour nozzles at low engine speeds, but at 11,500 rpm the efficiencies for the 7-gallon nozzles were slightly higher.

The first combustion-chamber basket modification with the holes of the third step blocked resulted in the lowest combustion efficiencies of all the engine modifications. This decrease was attributed to the increase in primary air and the introduction of secondary air further downstream than with the other combustion chambers. The combustion efficiency of the modified engine, with modified compressor and combustion chamber and with the 171-square-inch exhaust nozzle, was approximately 4 points higher than the combustion efficiency of the original engine over the entire range of engine speeds.

Pressure Losses

The engine-cycle efficiency of a turbojet engine is adversely affected by any loss in total pressure through the combustion chamber (reference 3). Thus the variation of combustion-chamber total-pressure loss with operating conditions is important to the over-all performance of the engine.

Variations of over-all total-pressure-loss ratio with engine speed for the modified engine are shown in figure 17 for a range of altitudes from 15,000 to 35,000 feet at flight Mach numbers of 0.71 and 0.52. An increase in altitude resulted in a reduction in the combustion-chamber total-pressure-loss ratio $\Delta P_T/P_4$ at engine speeds greater than 8000 rpm. Peak values of $\Delta P_T/P_4$ occurred in the low or medium engine-speed range.

The variation of $\Delta P_T/P_4$ with engine speed and flight Mach number is shown in figure 18 for the modified engine at simulated altitudes of 35,000 and 25,000 feet. Increasing the flight Mach number considerably increased the over-all total-pressure-loss ratio, particularly at engine speeds below 10,000 rpm. The maximum $\Delta P_T/P_4$ obtained with the modified engine was about 0.102 at an altitude of 25,000 feet, a flight Mach number of 1.05, and an engine speed of 8000 rpm (fig. 18(b)). These losses in total pressure through the combustion chamber are somewhat higher than those that have been obtained with cylindrical-type combustion chambers.

The effect of engine speed and exhaust-nozzle-outlet area on the modified-engine combustion-chamber total-pressure-loss ratio is shown in figure 19. The value of $\Delta P_T/P_4$ increased as the exhaust-nozzle area was increased over the entire range of engine speeds. With the 171-square-inch exhaust nozzle on the engine, a maximum $\Delta P_T/P_4$ of 0.070 was obtained at 25,000 feet with a flight Mach

number of 0.52. Installation of the 330-square-inch exhaust nozzle on the engine increased the maximum value of $\Delta P_T/P_4$ to 0.089 at the same altitude and flight Mach number.

The effect of various engine modifications on the over-all total-pressure-loss ratio is shown in figure 20. Blocking the third-step holes of the basket resulted in total-pressure-loss ratios as much as 23 percent higher than the losses obtained with the original basket. A slight reduction in $\Delta P_T/P_4$ was obtained by replacing the 7-gallon-per-hour nozzles with $7\frac{1}{2}$-gallon-per-hour nozzles; however, no appreciable effect on combustion-chamber pressure-loss characteristics was obtained by changing from 7- to 3-gallon fuel nozzles or by blocking one-half of the fuel nozzles.

Pressure losses for the modified engine, with modified compressor and combustion chamber and with the 171-square-inch exhaust nozzle, were lower than the pressure losses obtained with the other configurations. The maximum value of $\Delta P_T/P_4$ obtained with the modified engine at 35,000 feet and a flight Mach number of 0.52 was about 0.068 at 8500 rpm.

The effect of the combustion-chamber-inlet screens on the combustion-chamber total-pressure-loss ratio of the modified and the original engines is shown in figure 21. The inlet screens of 60- and 40-percent blocking area used on the original engine increased the loss in total pressure across the combustion chamber by about 2 percent of the compressor-outlet total pressure P_4. The 30-percent blocking-area screens used on the modified engine increased the combustion-chamber total-pressure loss by less than 1 percent of P_4 at high engine speeds.

The pressure-loss data did not lend itself to analysis with the type of pressure-loss chart constructed in reference 3. Failure of these data to correlate with the pressure-loss chart is attributed to changes of the flame characteristics, which caused the value of the combustion-chamber equivalent area A_b to vary. The value of the friction-pressure-loss factor K was determined for the original and modified combustion chambers from windmilling data with no burning in the engine. These values of K were approximately 0.027 and 0.024 for the original and modified combustion chambers, respectively. In the evaluation of K, the combustion-chamber-inlet screens were considered as part of the combustion chamber, and the difference in the value of K for the two combustion chambers is attributed to the difference in blocking area of the screens and the change in hole configuration.

Losses in Engine-Cycle Efficiency

The effect of altitude and engine speed on engine-cycle efficiency and the fractional loss in engine-cycle efficiency due to combustion-chamber pressure losses of the modified engine is shown in figure 22. At a given engine speed, the engine-cycle efficiency η increased with altitude. The fractional loss in engine-cycle efficiency $\Delta\eta/\eta$ due to combustion-chamber pressure losses decreased with an increase in altitude at a constant engine speed. Lowering the engine speed resulted in an increase in $\Delta\eta/\eta$ over the entire range of engine speeds, but the fractional loss was appreciable only in the low engine-speed region.

Variations of engine-cycle efficiency and fractional loss in engine-cycle efficiency with engine speed and flight Mach number are shown in figure 23 for the modified engine. At engine speeds greater than 10,000 rpm at an altitude of 25,000 feet, the engine-cycle efficiency varied directly with flight Mach number. The maximum engine-cycle efficiency obtained during the investigation was about 0.39 at an altitude of 25,000 feet, an engine speed of 12,500 rpm, and a flight Mach number of 1.05. An increase in flight Mach number resulted in a higher $\Delta\eta/\eta$ at low engine speeds, but the flight-Mach-number effect was negligible at engine speeds greater than 11,000 rpm. The lowest value of the fractional loss in engine-cycle efficiency obtained at 25,000 feet was about 0.04 at the maximum engine speed of 12,500 rpm.

The effect of exhaust-nozzle-outlet area on engine-cycle efficiency and fractional loss in engine-cycle efficiency at an altitude of 25,000 feet and a flight Mach number of 0.52 is shown in figure 24. Engine-cycle efficiency decreased considerably with increased exhaust-nozzle-outlet area. With the 171-square-inch exhaust nozzle installed on the engine, the engine-cycle efficiency was about 0.325 at 12,000 rpm. With an exhaust-nozzle area of 330 square inches, the engine-cycle efficiency at the same engine speed was only 0.105. Large exhaust-nozzle cross-sectional areas resulted in very high values of $\Delta\eta/\eta$.

The improvement in cycle efficiency and the reduction in fractional loss in engine-cycle efficiency that were obtained with the modified engine as compared with the original engine operating at a flight Mach number of 0.52 at an altitude of 35,000 feet is shown in figure 25. At an engine speed of 11,500 rpm, the engine-cycle efficiency was increased from 0.25 to 0.33 by modifying the engine. The value of $\Delta\eta/\eta$ at this engine speed was 0.08 for the original engine and 0.04 for the modified engine.

SUMMARY OF RESULTS

An altitude-wind-tunnel investigation of a 3000-pound-thrust axial-flow turbojet engine gave the following results on the performance characteristics of the annular-type combustion chamber:

1. Combustion efficiency varied directly with engine speed and, in general, inversely with altitude, flight Mach number, and exhaust-nozzle-outlet cross-sectional area. At altitudes up to 35,000 feet and at flight Mach numbers from 0.23 to 1.05, the maximum combustion efficiency of the modified engine varied from 0.95 to 0.99.

2. The combustion-chamber total-pressure-loss ratio $\Delta P_T/P_4$ varied directly with flight Mach number and exhaust-nozzle-outlet area and, in general, varied inversely with altitude. Maximum values of $\Delta P_T/P_4$ occurred at low or medium engine speeds. Lower values of $\Delta P_T/P_4$ were obtained with the modified engine than with the other configurations.

3. Engine-cycle efficiency varied directly with engine speed and altitude and inversely with exhaust-nozzle-outlet area. At high engine speeds, the engine-cycle efficiency varied directly with flight Mach number. The engine-cycle efficiency of the modified engine was considerably higher than that obtained with the original engine.

4. The fractional loss in engine-cycle efficiency due to combustion-chamber pressure losses $\Delta\eta/\eta$ varied inversely with engine speed and altitude. With the 171-square-inch exhaust nozzle, $\Delta\eta/\eta$ was appreciable only at low engine speeds. At low engine speeds, $\Delta\eta/\eta$ varied directly with flight Mach number, but at high engine speeds there was no appreciable variation. Engine operation with large exhaust-nozzle-outlet areas resulted in very high fractional losses in cycle efficiency.

Flight Propulsion Research Laboratory,
National Advisory Committee for Aeronautics,
Cleveland, Ohio.

925

APPENDIX - CALCULATIONS

Symbols

The following symbols are used in this report:

A cross-sectional area, sq ft

c_p specific heat at constant pressure, Btu/(lb)(°R)

f/a fuel-air ratio

g acceleration of gravity, 32.17 ft/sec^2

h enthalpy, Btu/lb

J mechanical equivalent of heat, 778 ft-lb/Btu

K combustion-chamber friction-pressure-loss factor

N rotational speed of engine, rpm

P total pressure, lb/sq ft absolute

ΔP_F loss in total pressure in combustion chamber due to friction, lb/sq ft

ΔP_T over-all loss in total pressure in combustion chamber due to friction and heat addition, lb/sq ft

p static pressure, lb/sq ft absolute

R gas constant, 53.3 ft-lb/(lb)(°R)

T total temperature, °R

T_i indicated temperature, °R

t static temperature, °R

W mass flow through engine, lb/sec

γ ratio of specific heat at constant pressure to specific heat at constant volume

η engine-cycle efficiency

$\Delta\eta$ loss in engine-cycle efficiency resulting from combustion-chamber pressure losses

η_b combustion efficiency

ρ air density, lb/cu ft

925

Subscripts:

0 free stream

1 cowl inlet

2 compressor inlet

4 combustion-chamber inlet or compressor outlet

4a combustion-chamber inlet behind screens

5 combustion-chamber outlet or turbine inlet

7 turbine outlet

8 exhaust-nozzle outlet

a air

b combustion chamber

j station at which static pressure in jet reaches free-stream static pressure

Methods of Calculation

Temperature. - Static temperatures were obtained from indicated temperature readings by

$$t = \frac{T_i}{1 + 0.85\left[\left(\frac{P}{p}\right)^{\frac{\gamma-1}{\gamma}} - 1\right]}$$

where 0.85 is the thermocouple impact recovery factor.

The equivalent free-stream static temperature t_0 was calculated from the compressor-inlet indicated temperature as follows:

$$t_0 = T_2 \left(\frac{p_0}{P_2}\right)^{\frac{\gamma-1}{\gamma}}$$

925

The static temperature of the exhaust-gas jet was calculated from the tail-rake instrumentation by

$$t_j = t_8 \left(\frac{p_0}{p_8}\right)^{\frac{\gamma-1}{\gamma}}$$

No thermocouples were installed at the turbine inlet (station 5); in the determination of T_5, the enthalpy drop across the turbine was therefore assumed equal to the measured enthalpy rise through the compressor. The turbine enthalpy change and the turbine-outlet temperature T_7 were then used to obtain T_5 from a temperature-enthalpy chart.

Air flow. - Air-flow calculations were made from temperature and pressure measurements at the cowl inlet (station 1) by means of the equation

$$W_a = \frac{p_1 A_1}{R} \sqrt{\frac{2gJc_p}{t_1}\left[\left(\frac{P_1}{p_1}\right)^{\frac{\gamma-1}{\gamma}} - 1\right]}$$

where the value of A_1 is 1.78 square feet.

Combustion efficiency. - The enthalpy of the gas at the turbine inlet can be expressed as

$$(1 + f/a)\, h_5 = h_{a,5} + f/a \left(\frac{Am + B}{m + 1}\right)$$

where the first term on the right-hand side of the equation is the enthalpy of the air and the second term is the enthalpy of the fuel as presented in reference 4. (The symbols A, m, and B are defined in this reference.) The combustion efficiency is defined as the ratio of the actual increase in enthalpy of the gas while passing through the combustion chamber to the theoretical increase

in enthalpy that would result from complete combustion of the fuel charge. When a fuel with a lower heating value of 19,370 Btu per pound is used, the following expression for combustion efficiency is obtained:

$$\eta_b = \frac{h_{a,5} + f/a\left(\frac{Am + B}{m + 1}\right) - h_{a,4}}{(f/a) \times 19,370}$$

925

The values in this equation were obtained from a temperature-enthalpy chart based on a fuel-inlet temperature of 80° F and a hydrogen-carbon ratio of the fuel of 0.170.

Pressure losses. - The total-pressure-loss ratio was calculated from total-pressure measurements at the combustion-chamber inlet and the combustion-chamber outlet according to the expression

$$\frac{\Delta P_T}{P_4} = \frac{P_4 - P_5}{P_4}$$

The friction-pressure-loss factor K for the original and revised combustion chambers was determined from engine windmilling tests. The total-pressure losses obtained resulted from friction alone inasmuch as there was no momentum pressure loss from heat addition (reference 3). The friction-pressure-loss factor K is defined by the relation

$$\Delta P_F = \frac{KW^2}{\rho}$$

Therefore,

$$K = \left(\frac{\Delta P_F}{P_4}\right)\left(\frac{P_4{}^2}{RW_a{}^2\ T_4}\right) = \frac{P_4\ (P_4 - P_5)}{RW_a{}^2\ T_4}$$

Windmilling tests were not made for all the engine modifications and therefore K could not be determined for those configurations.

Engine-cycle efficiency. - The engine-cycle efficiency is defined by

$$\eta = \frac{\text{heat supplied by source - heat rejected to sink}}{\text{heat supplied by source}}$$

$$\eta = \frac{\left[h_{a,5} + f/a\left(\frac{Am + B}{m + 1}\right) - h_{a,4}\right] - c_p\,(t_j - t_0)}{\left[h_{a,5} + f/a\left(\frac{Am + B}{m + 1}\right) - h_{a,4}\right]}$$

where c_p is the average value between stations j and 0.

The loss in engine-cycle efficiency resulting from combustion-chamber pressure losses was calculated by the expression

$$\Delta\eta = \frac{c_p\,t_j\left[1 - \left(\frac{P_5}{P_4}\right)^{\frac{\gamma-1}{\gamma}}\right]}{\left[h_{a,5} + f/a\left(\frac{Am + B}{m + 1}\right) - h_{a,4}\right]}$$

where c_p is the average value between stations j and 0.

REFERENCES

1. Dietz, Robert O., Jr., Berdysz, Joseph J., and Howard, Ephraim M.: Altitude-Wind-Tunnel Investigation of a 3000-Pound-Thrust Axial-Flow Turbojet Engine. II - Analysis of Compressor Performance. NACA RM No. E8A26a, 1948.

2. Conrad, Earl W., Dietz, Robert O., Jr., and Golladay, Richard L.: Altitude-Wind-Tunnel Investigation of a 3000-Pound-Thrust Axial-Flow Turbojet Engine. I - Analysis of Turbine Performance. NACA RM No. E8A23, 1948.

3. Pinkel, I. Irving, and Shames, Harold: Analysis of Jet-Propulsion Engine Combustion-Chamber Pressure Losses. NACA TN No. 1180, 1947.

4. Turner, L. Richard, and Lord, Albert M.: Thermodynamic Charts for the Computation of Combustion and Mixture Temperatures at Constant Pressure. NACA TN No. 1086, 1946.

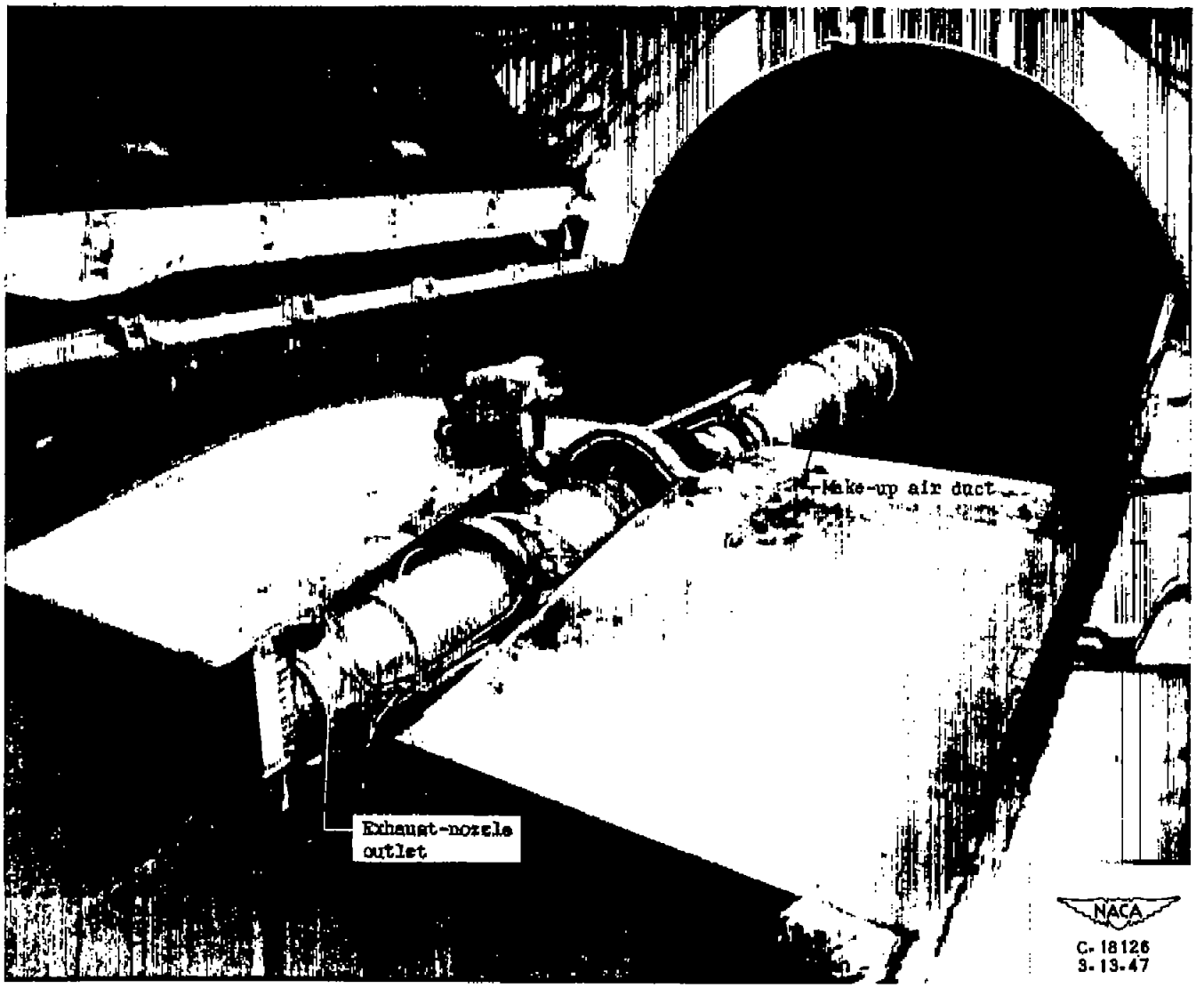

Figure 1. - Installation of turbojet engine in altitude wind tunnel.

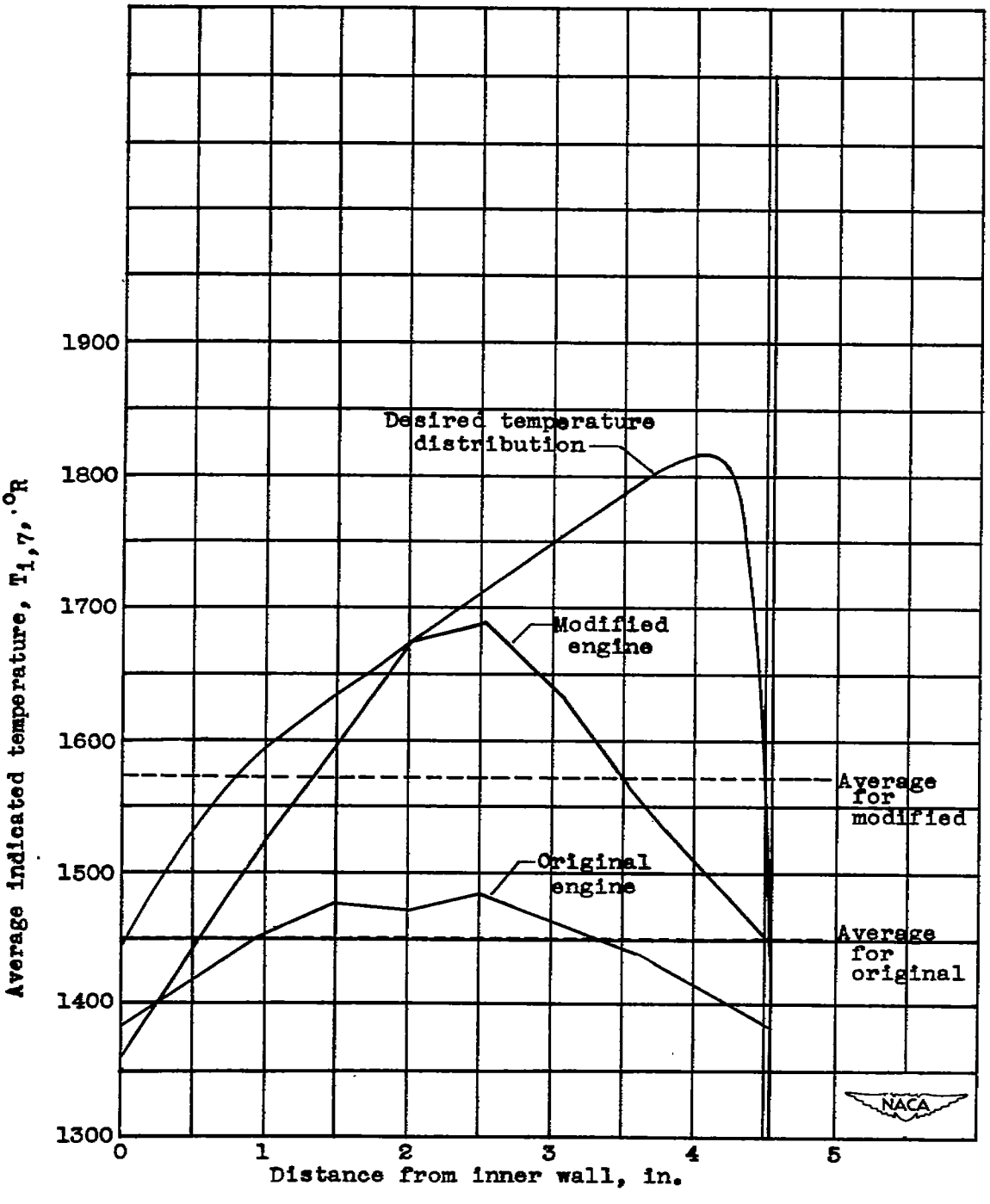

Figure 2. - Comparison of average temperature patterns at turbine outlet for original and modified engines at maximum engine speed and relation to manufacturer's desired temperature distribution as calculated from blade-stress considerations.

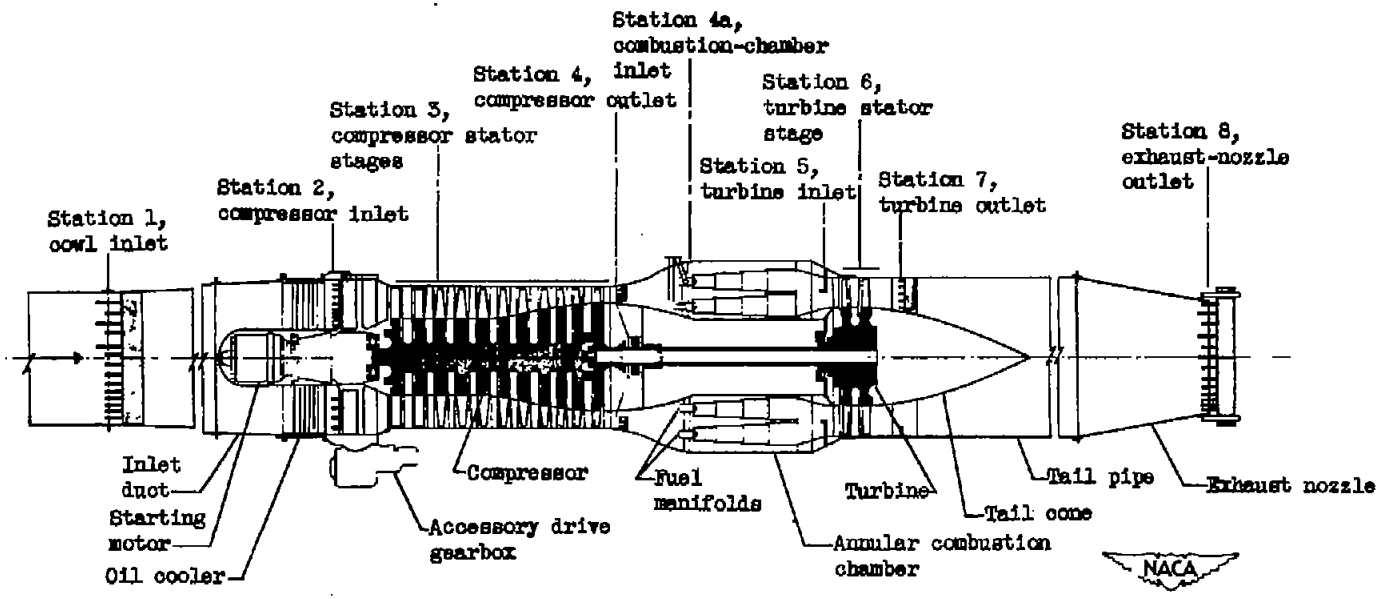

Figure 3. - Cross section of turbojet engine showing instrumentation stations.

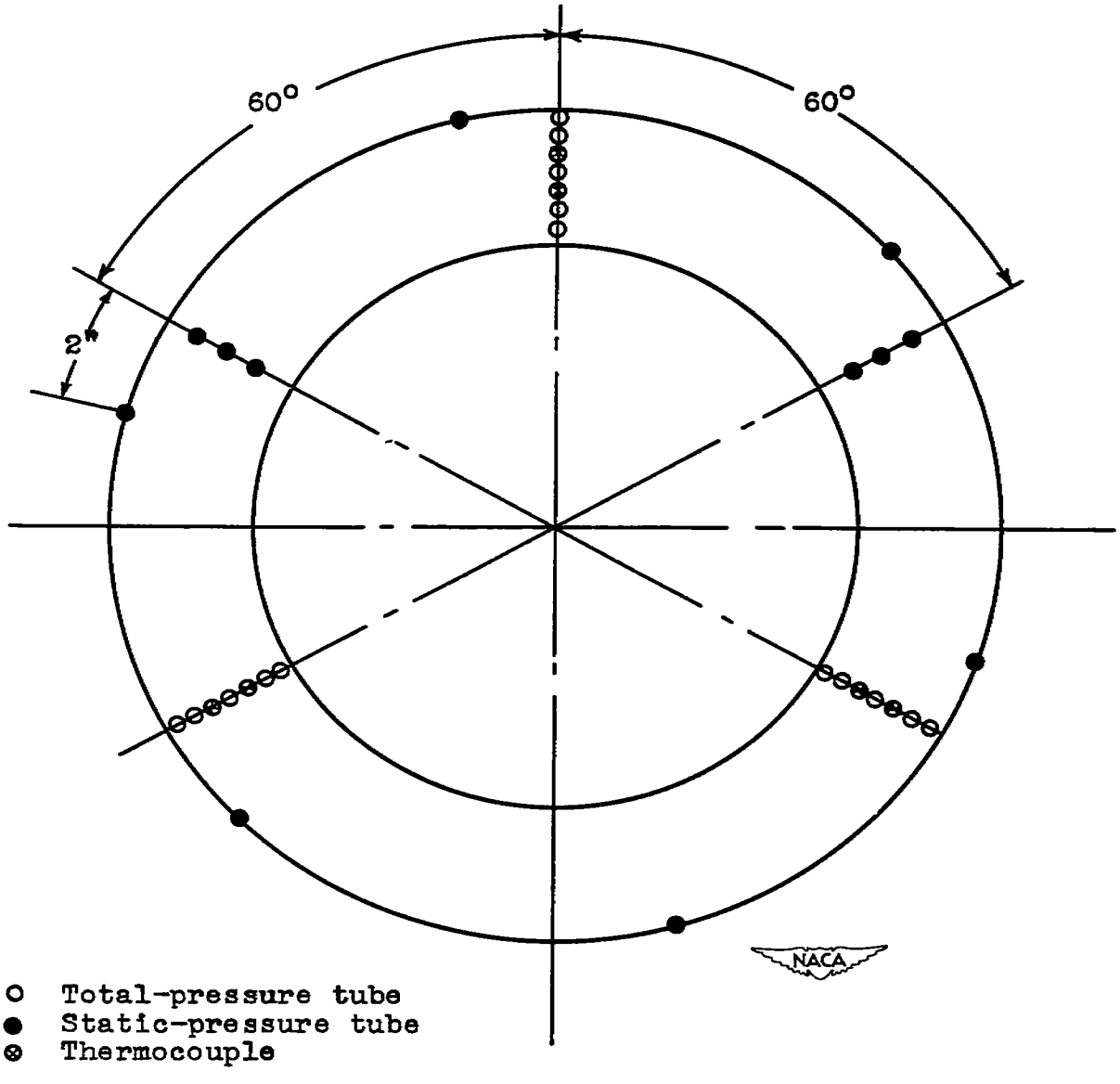

Figure 4. - Instrumentation at combustion-chamber inlet, station 4, $1\frac{1}{2}$ inches behind trailing edge of compressor-outlet straightening vanes.

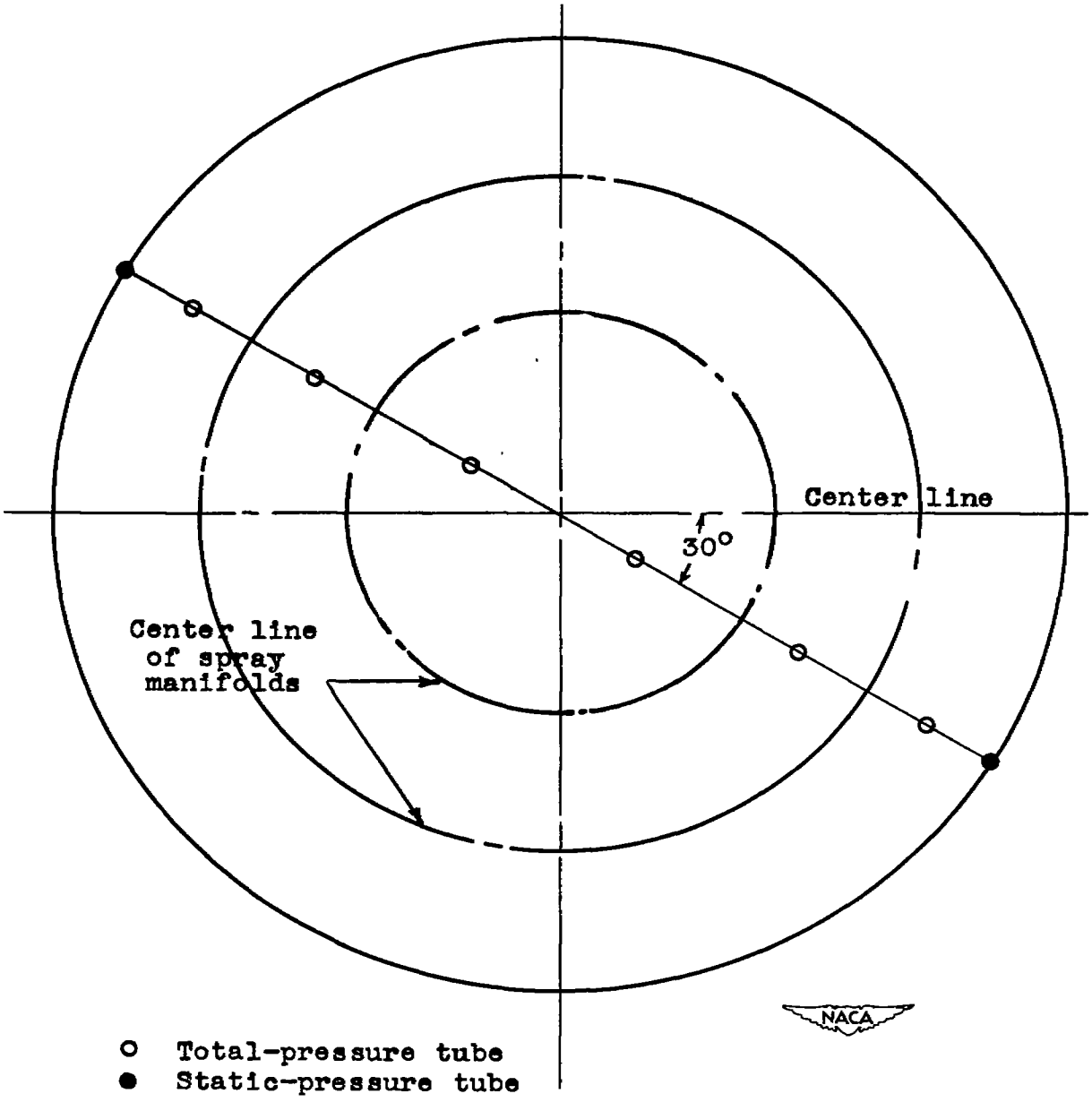

Figure 5. - Instrumentation at combustion-chamber inlet, station 4a, 1 inch behind combustion-chamber-inlet screens.

925

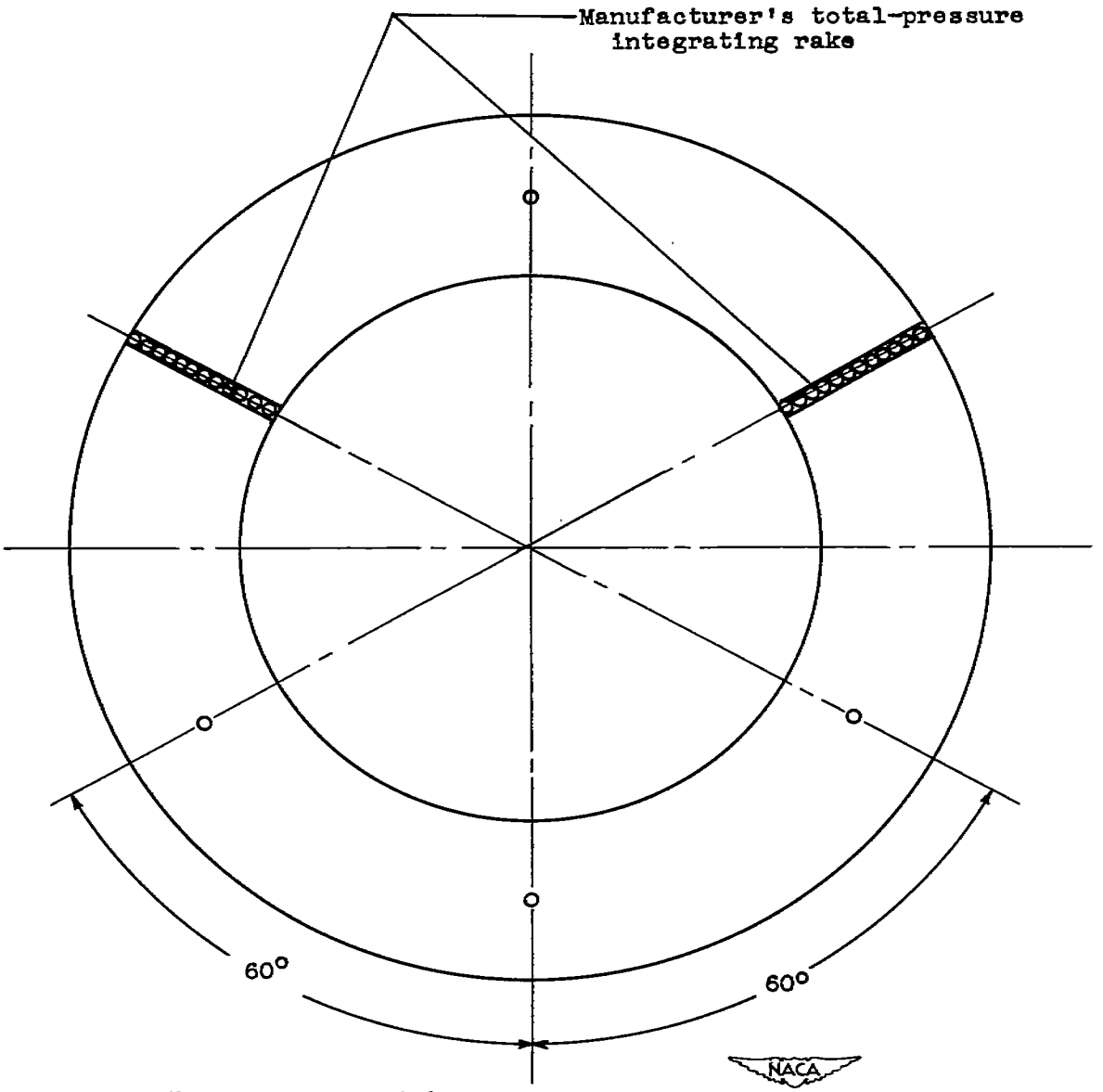

o Total-pressure tube

Figure 6. - Instrumentation at combustion-chamber outlet, station 5, $2\frac{3}{4}$ inches in front of center line of first-stage turbine stator blade.

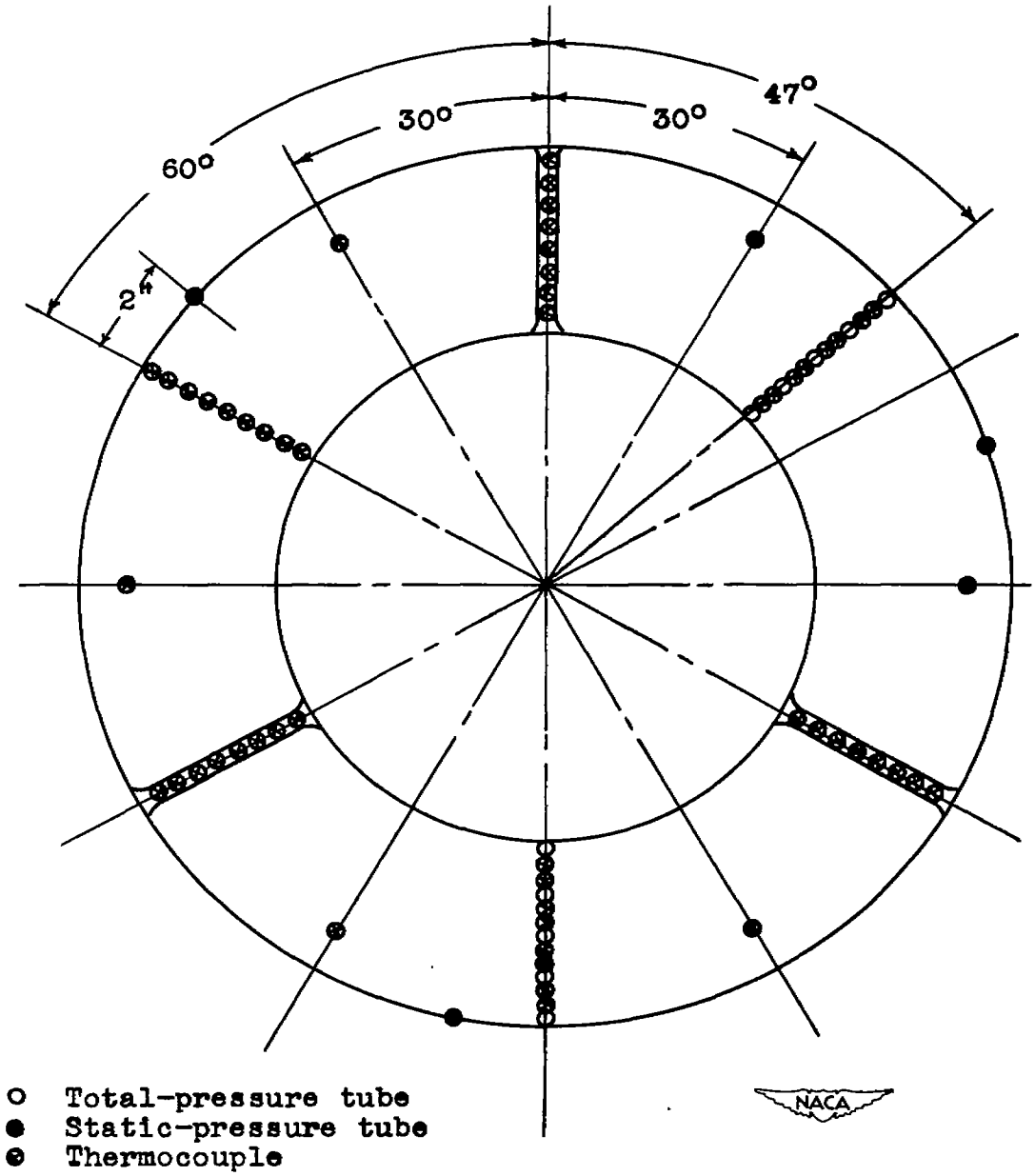

Figure 7. - Instrumentation at turbine outlet, station 7, $3\frac{3}{4}$ inches behind rear flange of turbine casing.

925

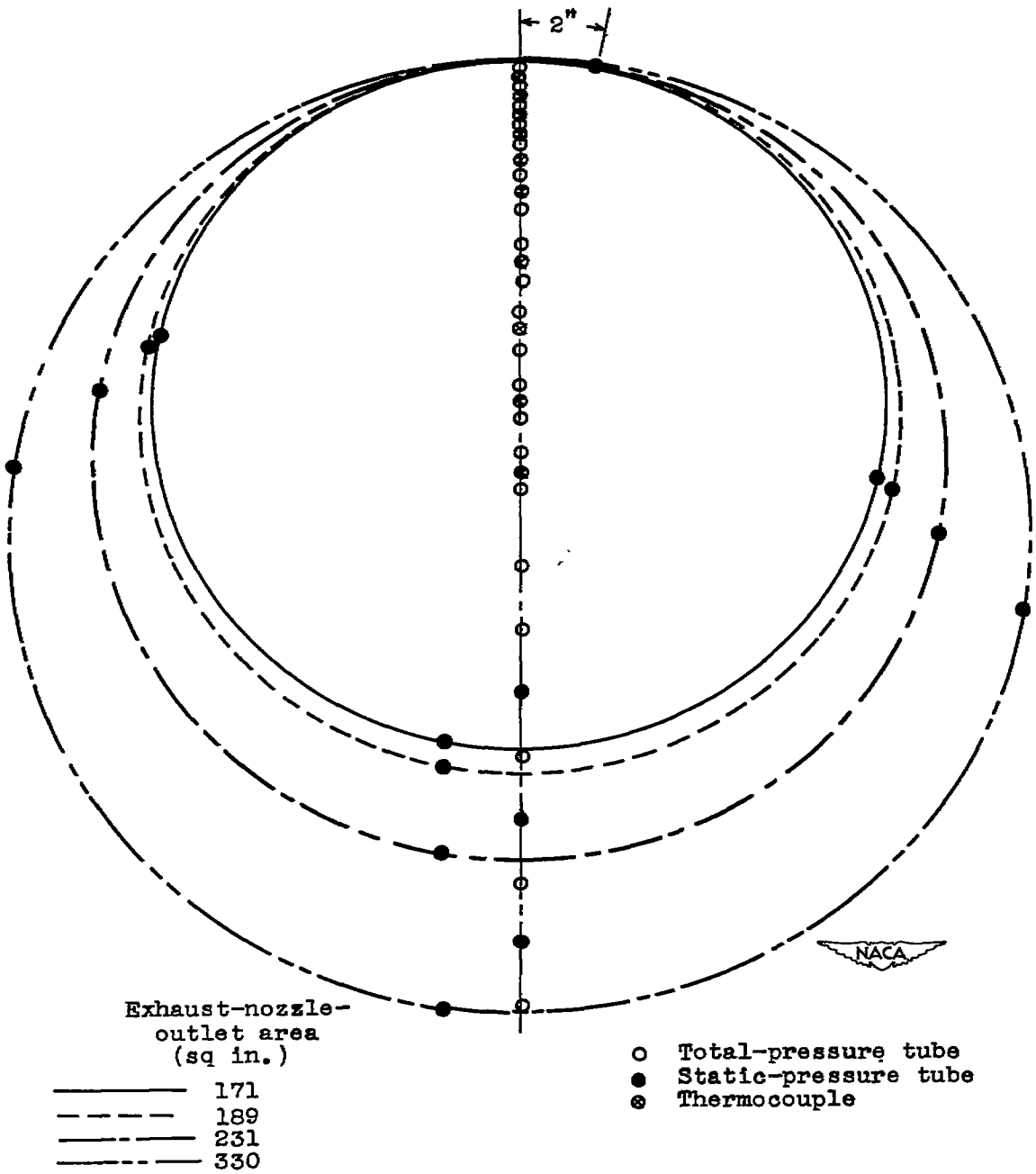

Figure 8. - Instrumentation at exhaust-nozzle outlet, station 8, 1 inch in front of rear edge of exhaust-nozzle outlet.

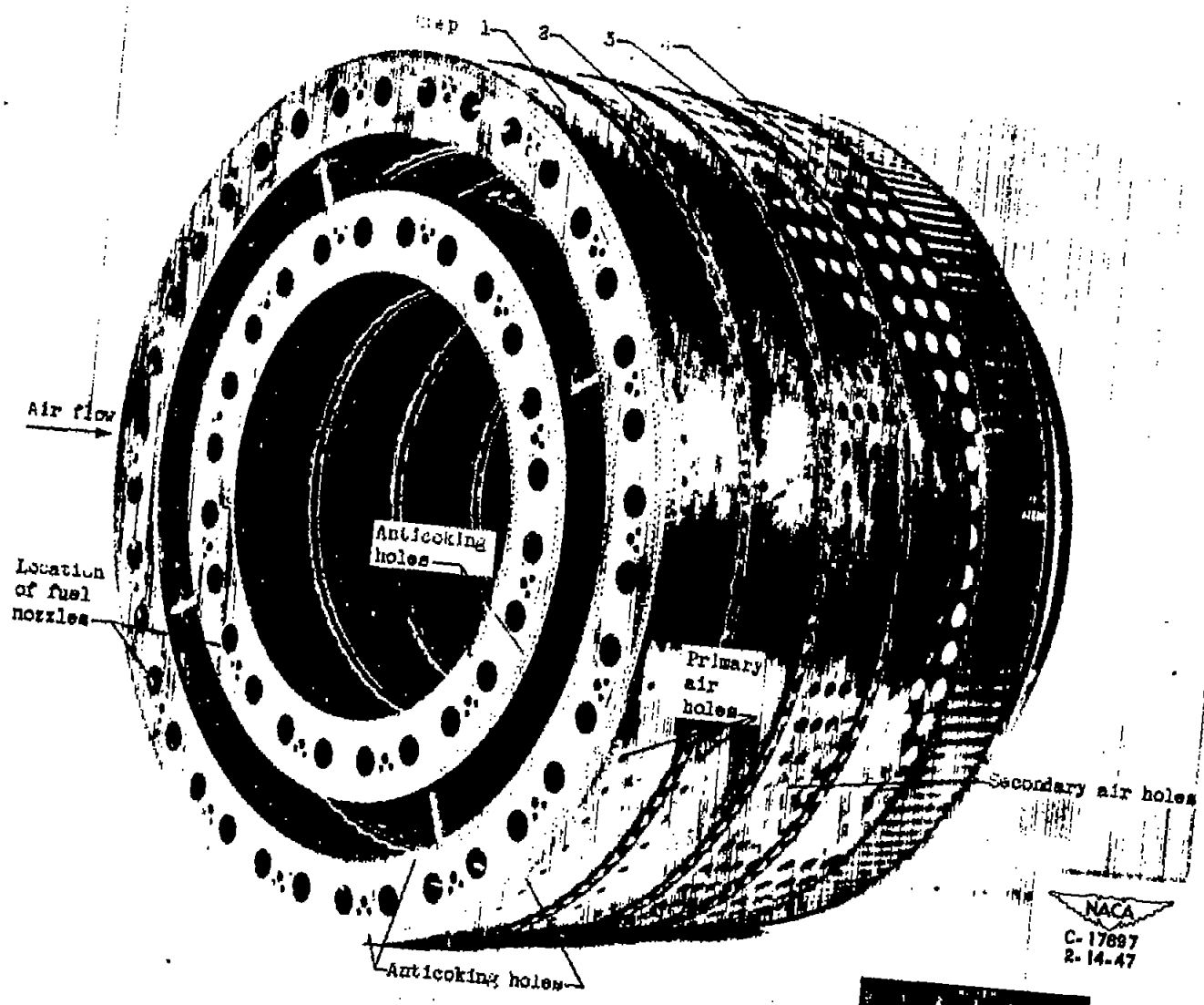

Figure 9. - Original combustion-chamber basket.

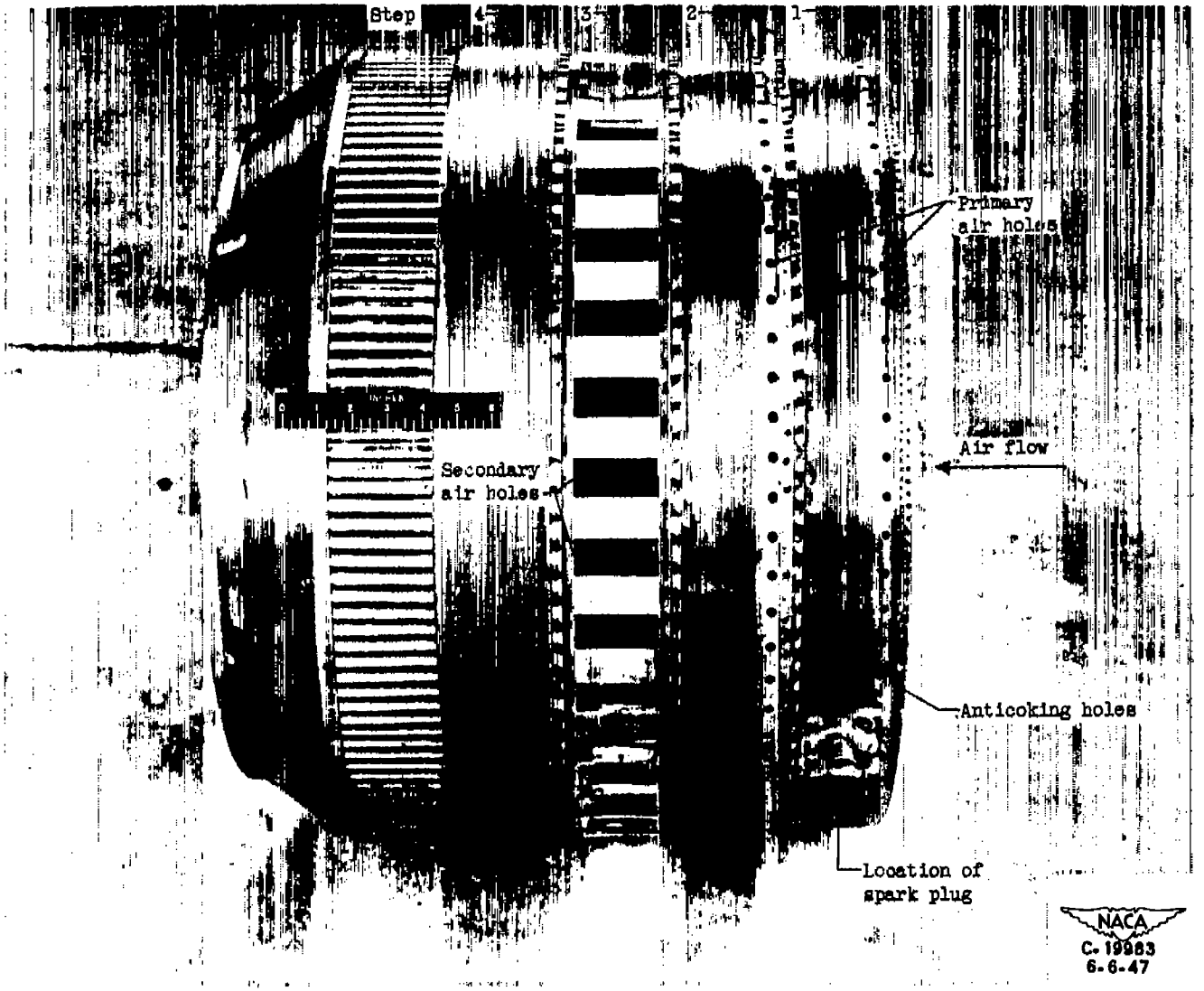

Figure 10. - Modified combustion-chamber basket with rectangular holes in third step and holes removed from fourth step.

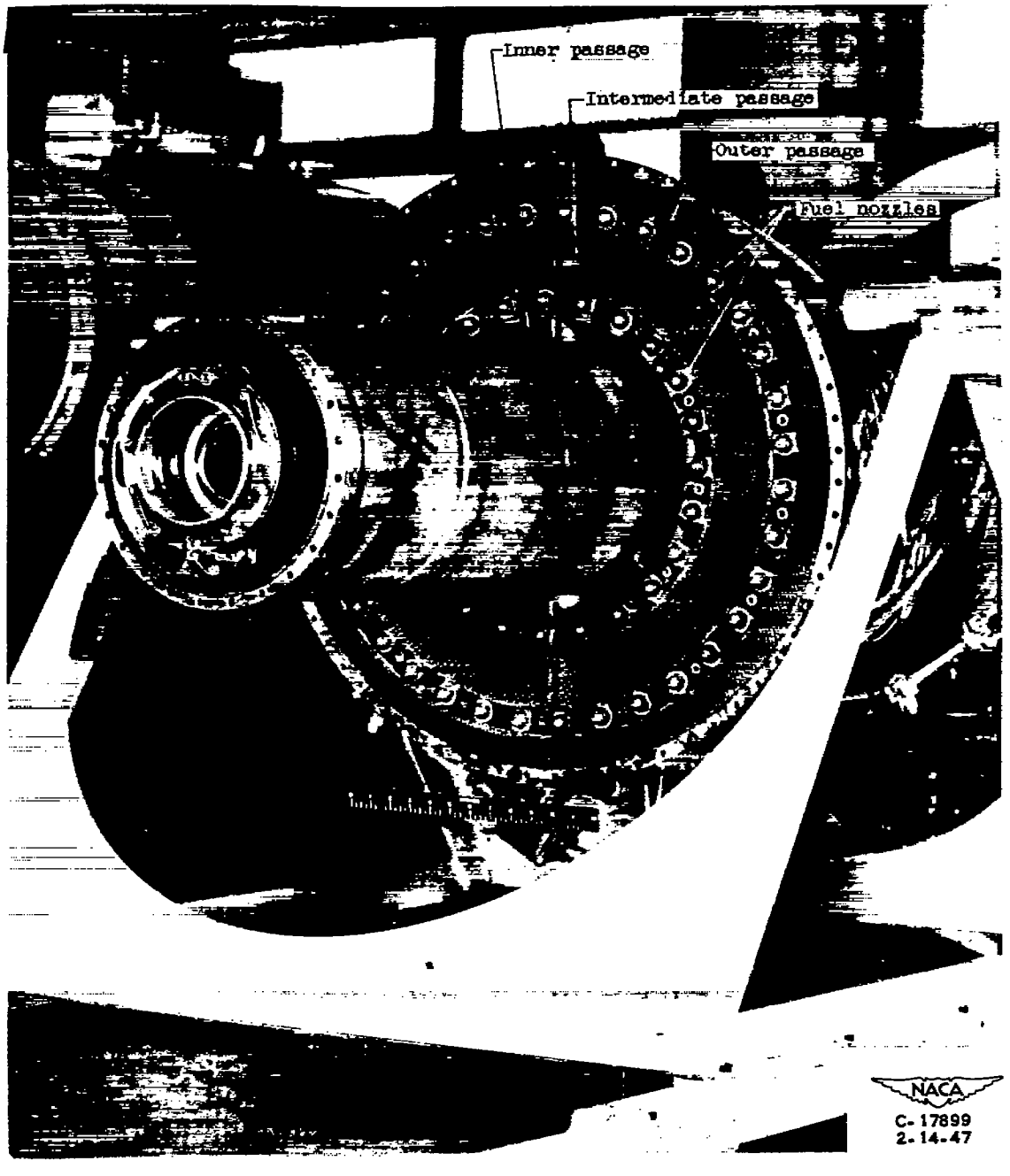

Figure 11. - Installation of combustion-chamber-inlet screens and fuel nozzles.

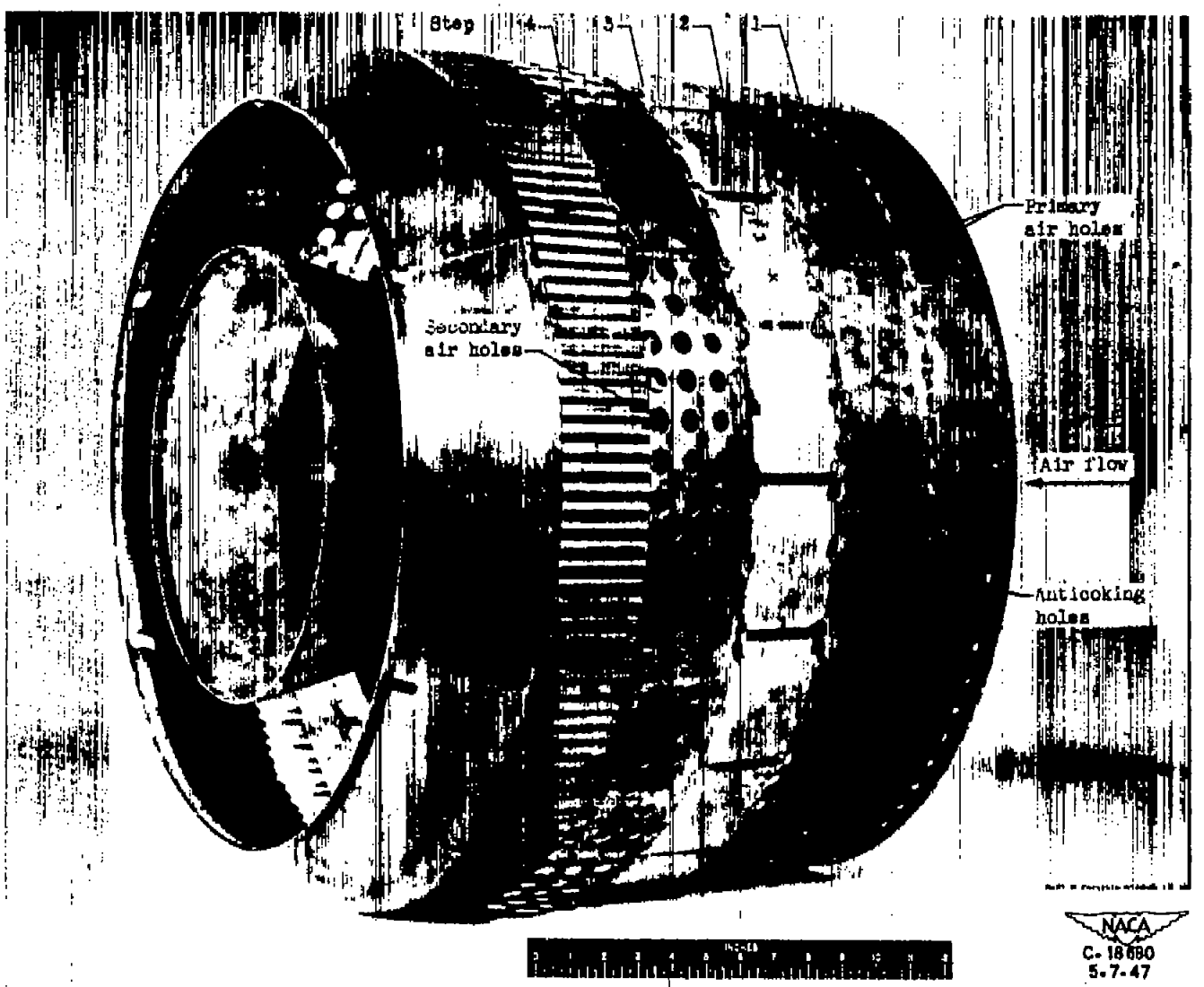

Figure 12. - Combustion-chamber basket with third-step holes blocked.

925

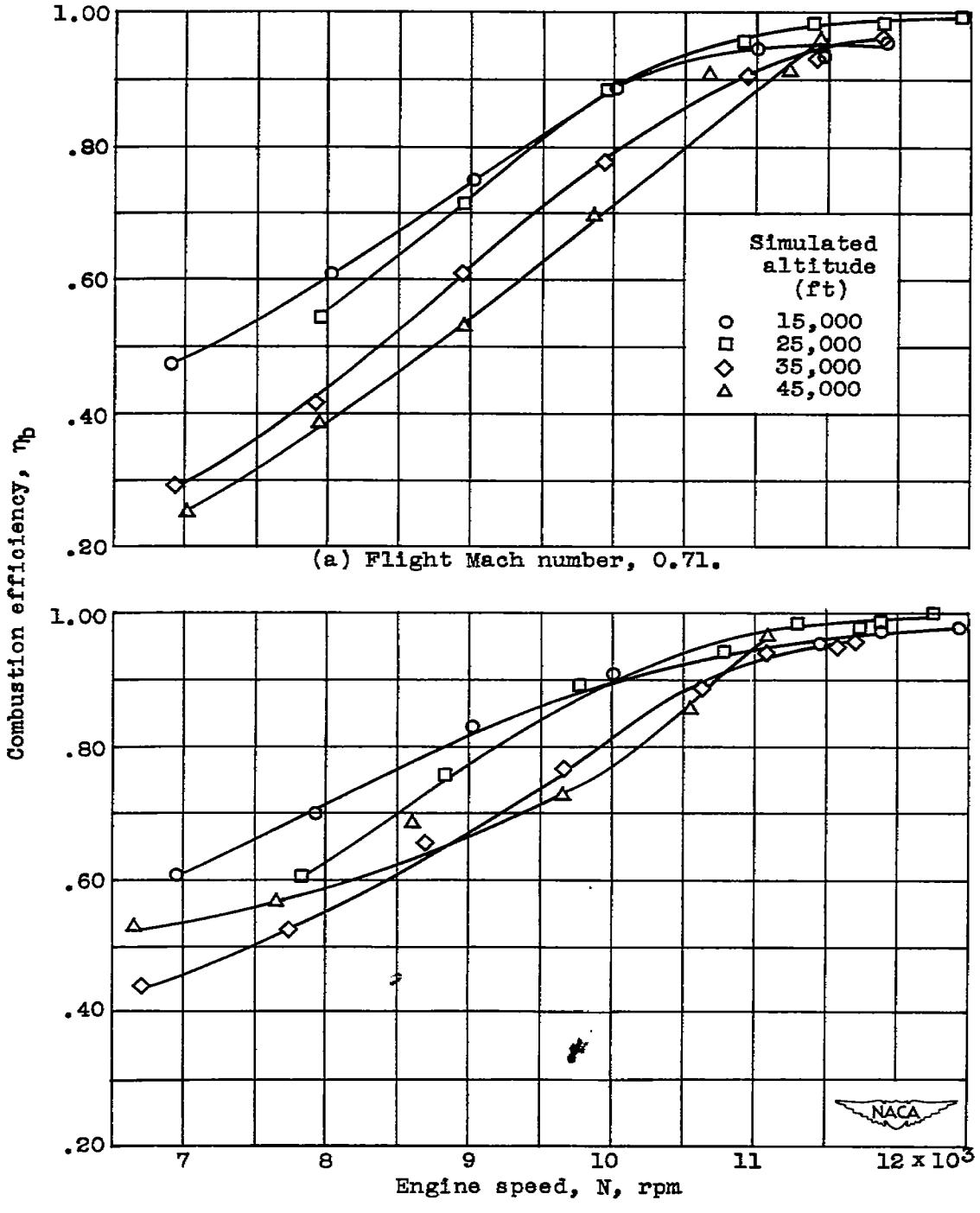

(a) Flight Mach number, 0.71.

(b) Flight Mach number, 0.52.

Figure 13. - Effect of engine speed and altitude on combustion efficiency of modified engine at flight Mach numbers of 0.52 and 0.71.

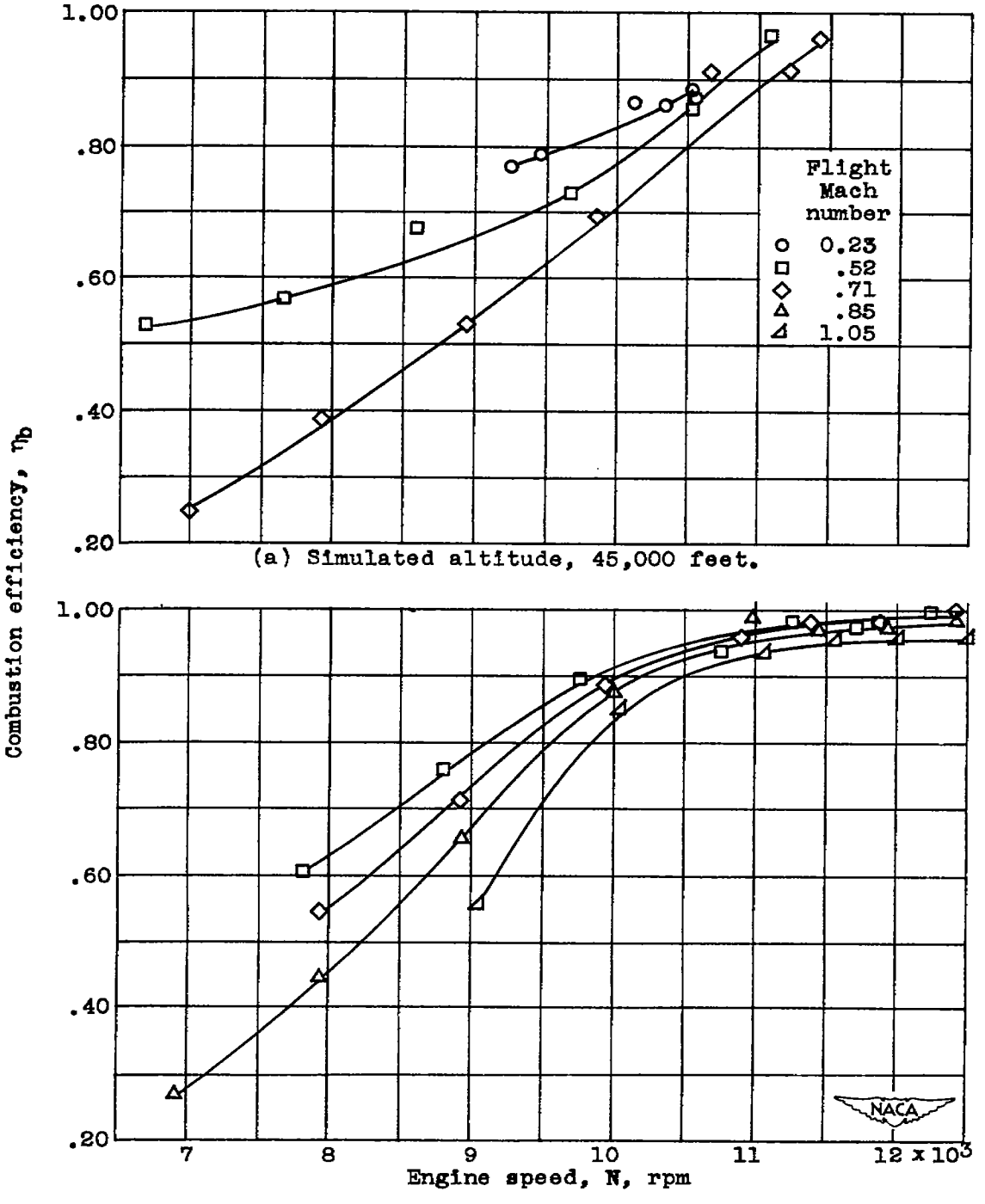

(b) Simulated altitude, 25,000 feet.

Figure 14. - Effect of engine speed and flight Mach number on combustion efficiency of modified engine at altitudes of 25,000 and 45,000 feet.

[redacted]

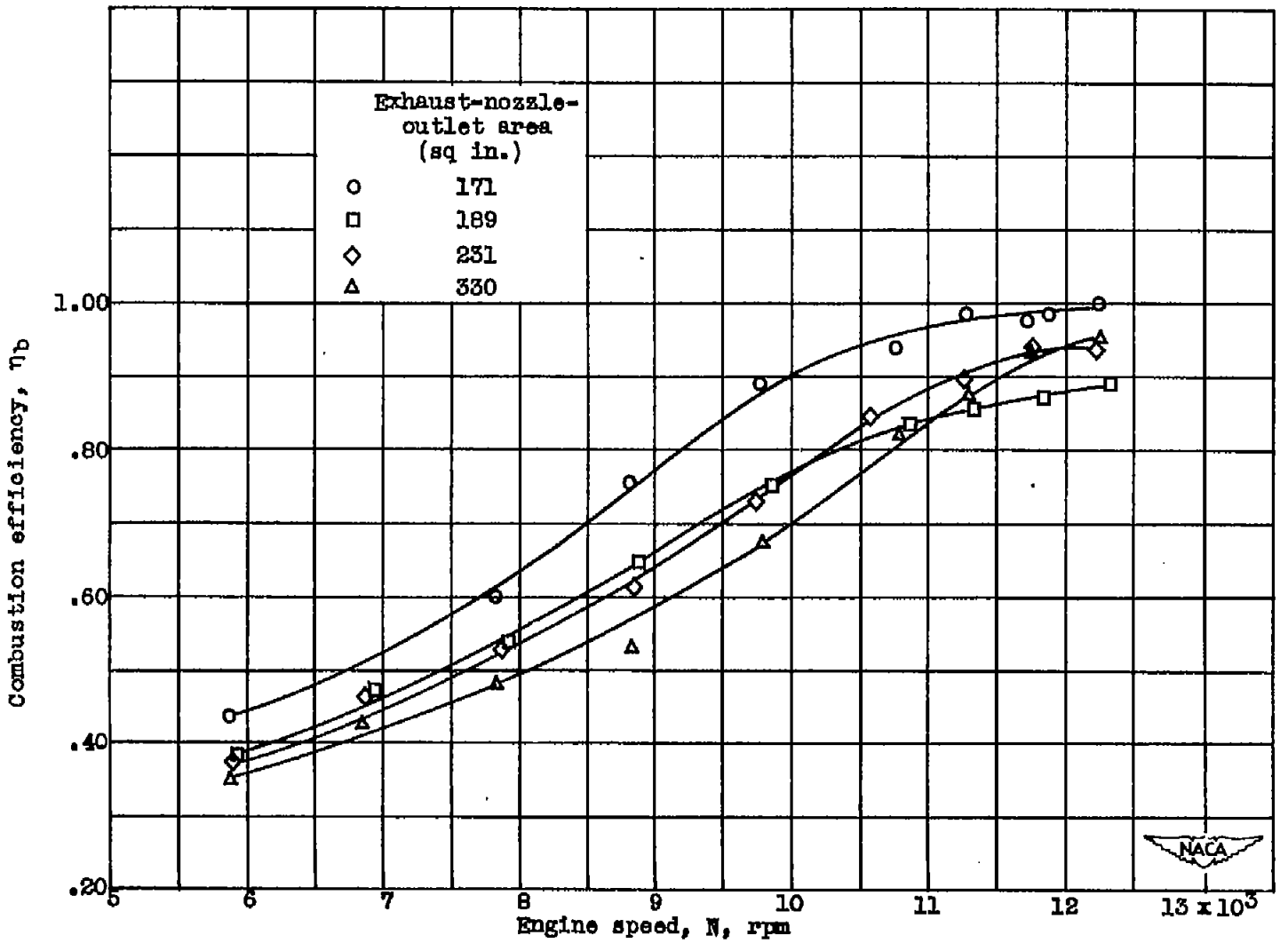

Figure 15. - Effect of engine speed and exhaust-nozzle-outlet area on combustion efficiency of modified engine at altitude of 25,000 feet and flight Mach number of 0.52.

[redacted]

[redacted]

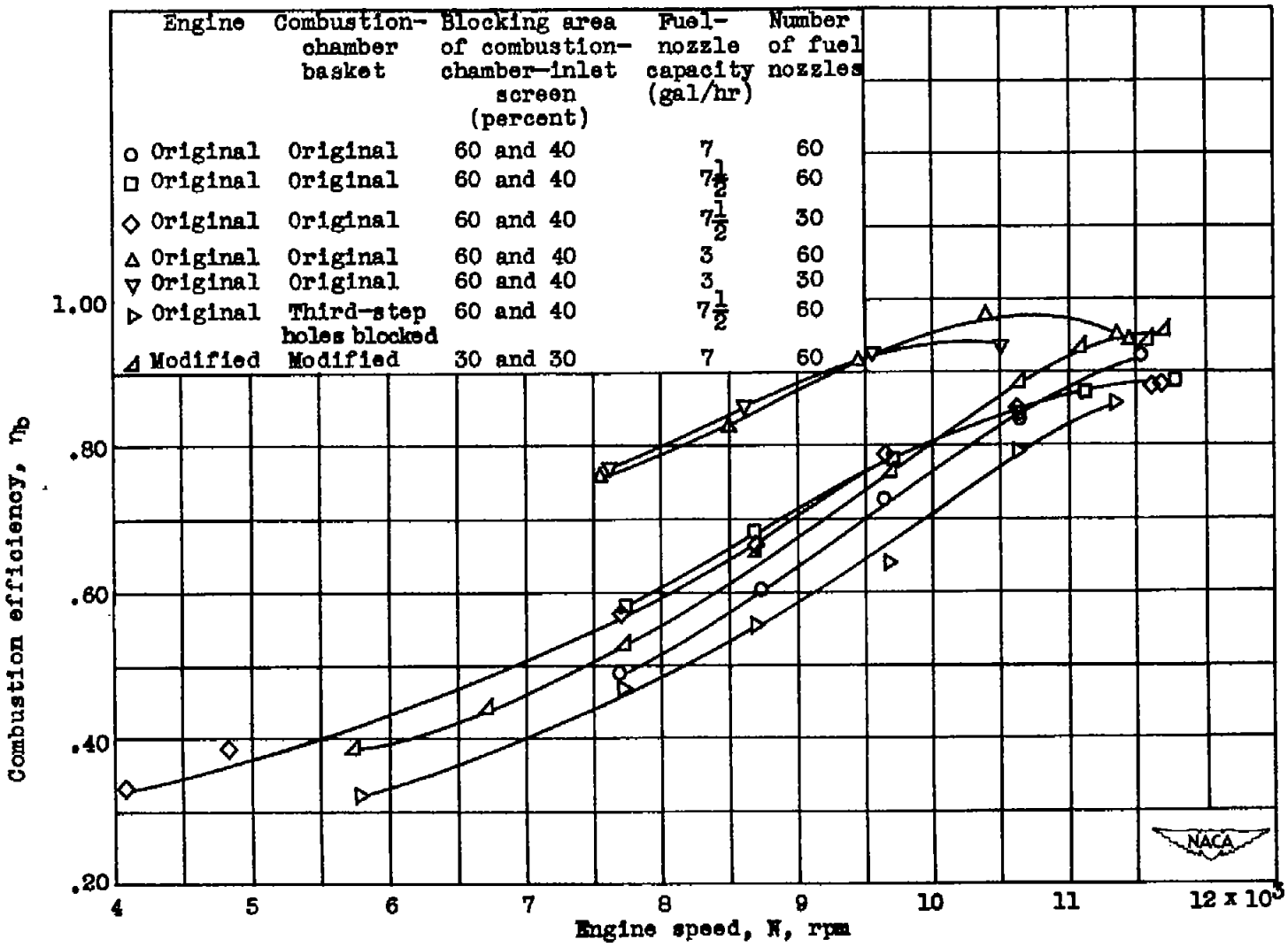

Figure 16. - Effect of engine speed on combustion efficiency for various modifications of original engine and for modified engine at altitude of 35,000 feet and flight Mach number of 0.52.

[redacted]

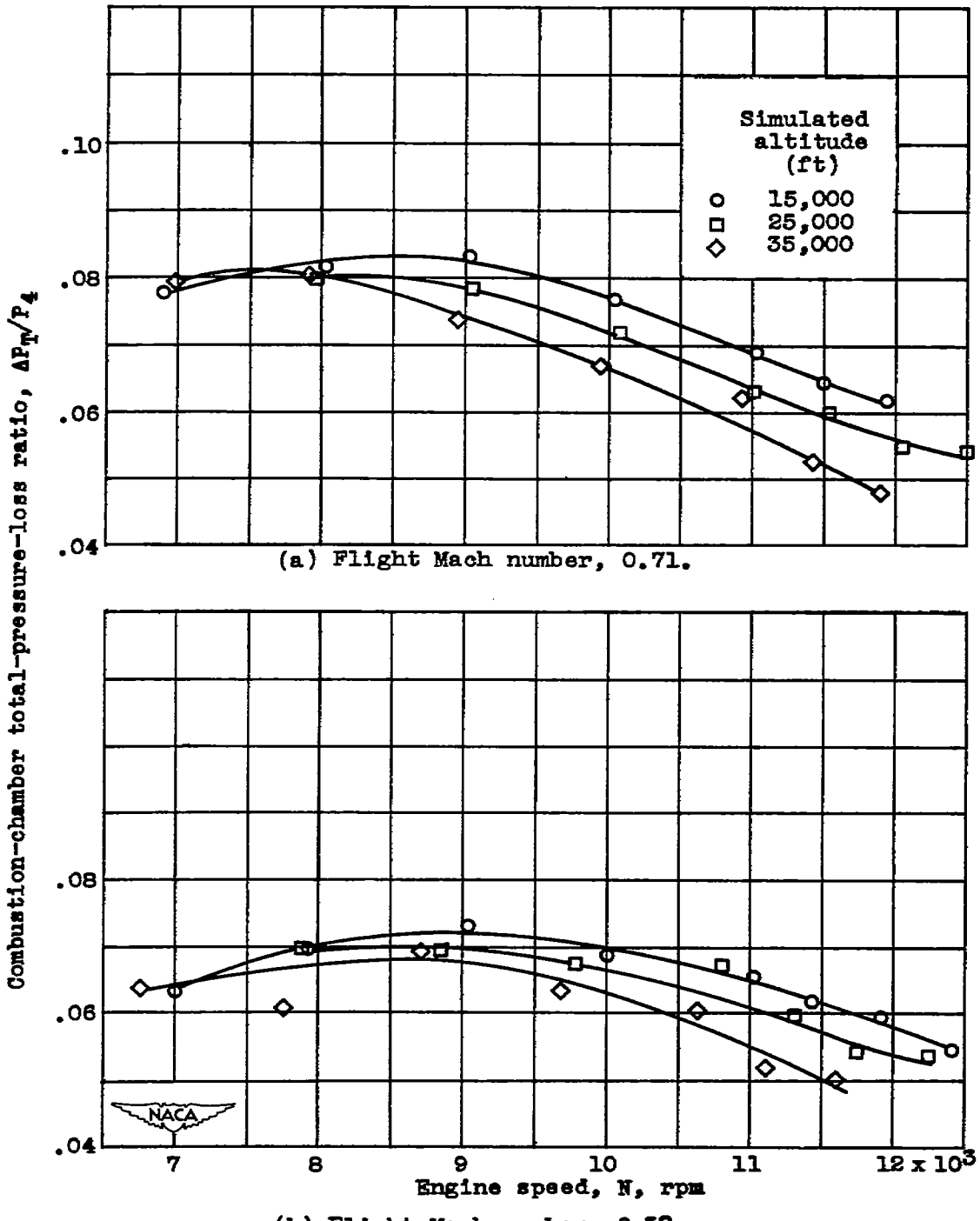

(b) Flight Mach number, 0.52.

Figure 17. - Effect of engine speed and altitude on over-all total-pressure-loss ratio through combustion chamber of modified engine at flight Mach numbers of 0.52 and 0.71.

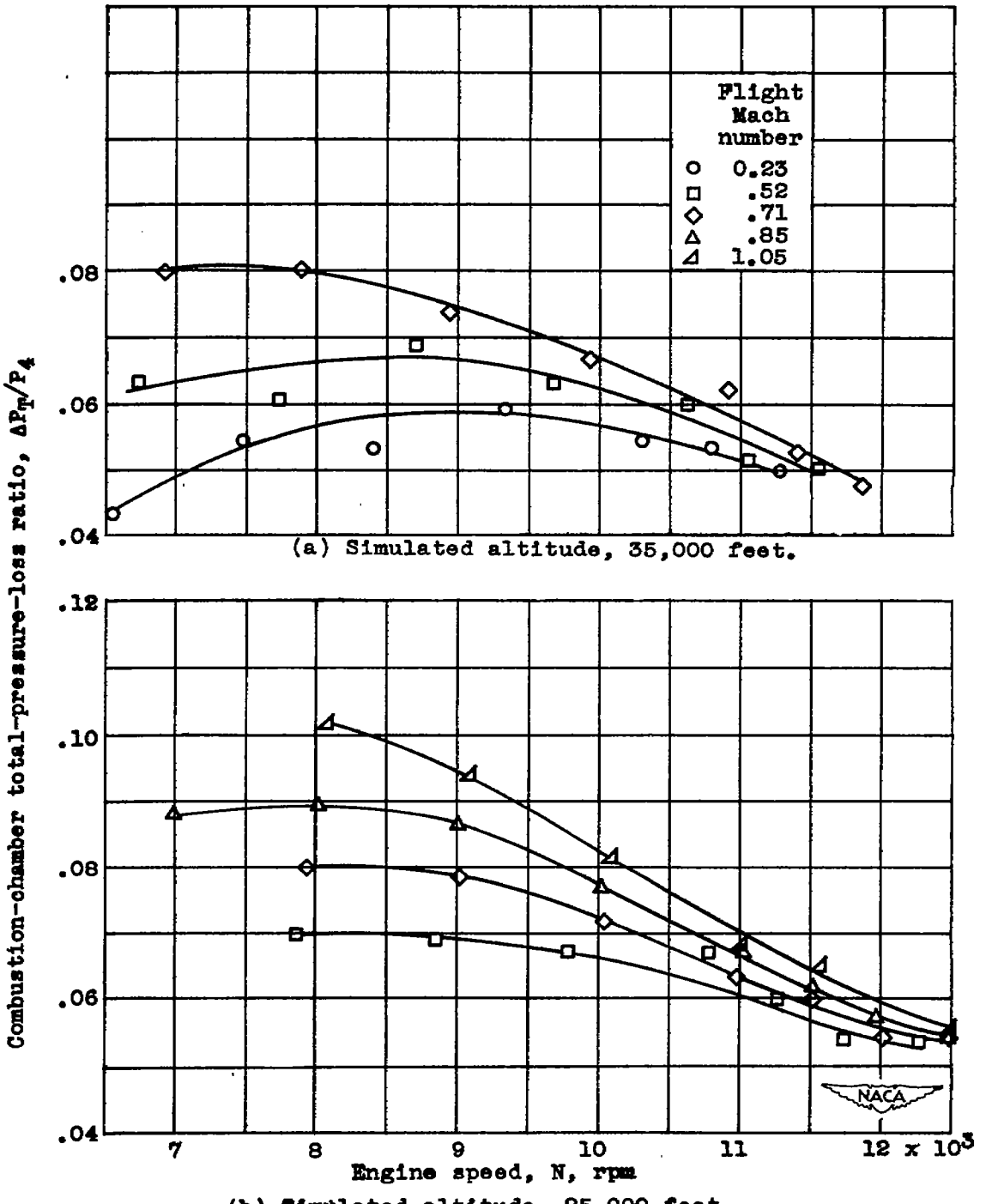

(b) Simulated altitude, 25,000 feet.

Figure 18. - Effect of engine speed and flight Mach number on over-all total-pressure-loss ratio through combustion chamber of modified engine at altitudes of 25,000 and 35,000 feet.

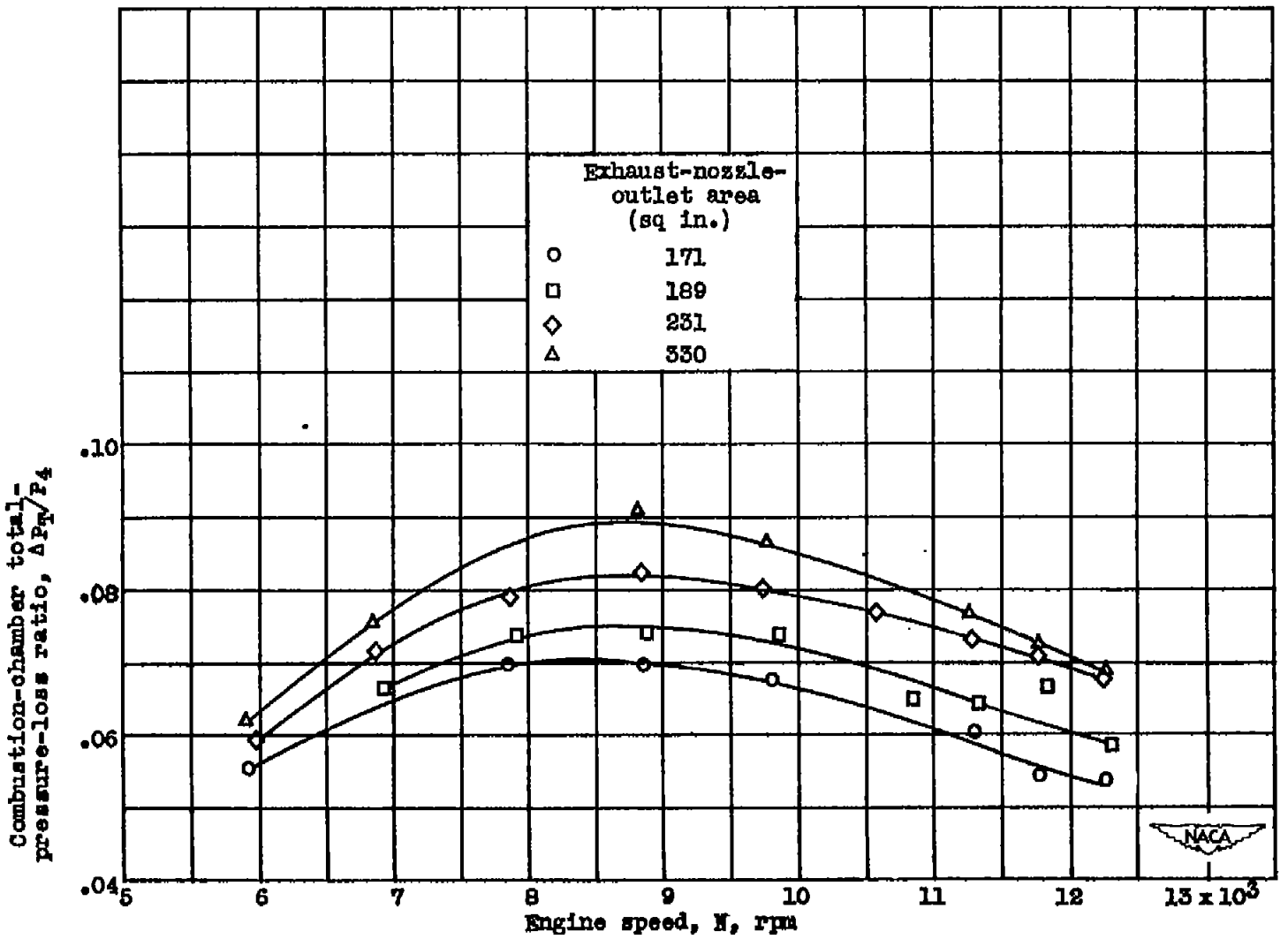

Figure 19. - Effect of engine speed and exhaust-nozzle-outlet area on over-all total-pressure-loss ratio through combustion chamber of modified engine at altitude of 25,000 feet and flight Mach number of 0.52.

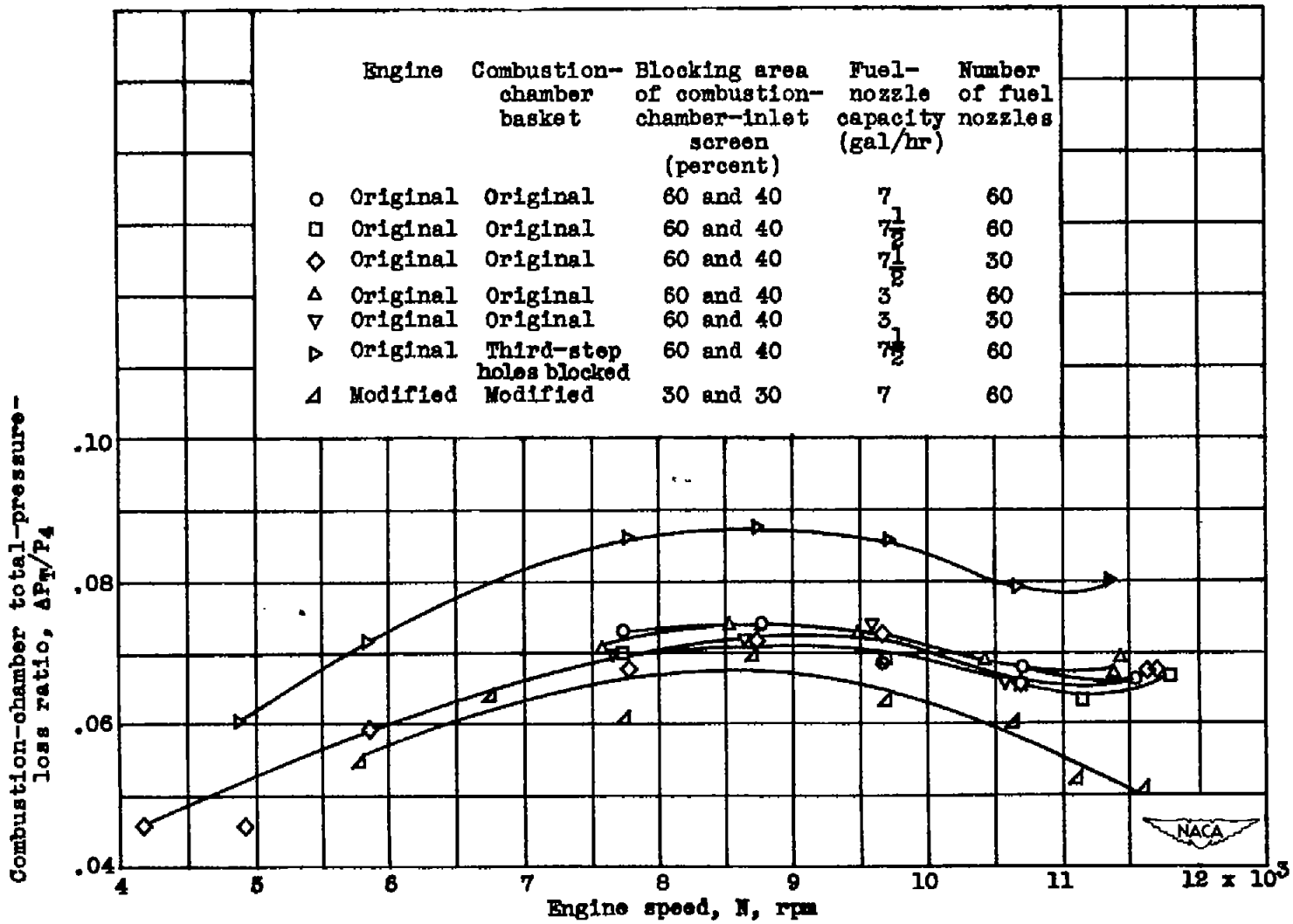

Figure 20. - Effect of engine speed on combustion-chamber total-pressure-loss ratio for various modifications of original engine and for modified engine at altitude of 35,000 feet and flight Mach number of 0.52.

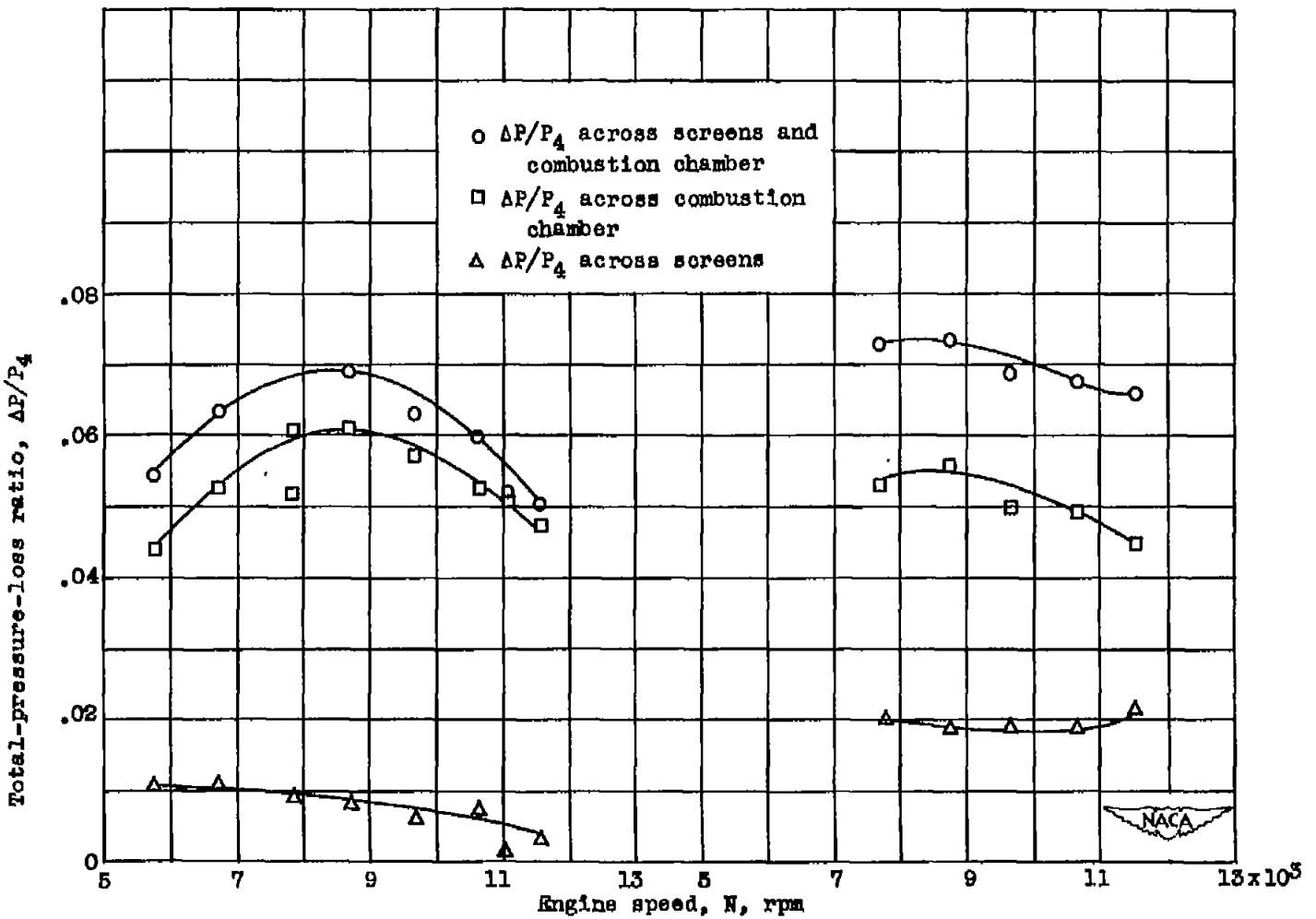

(a) Modified engine; combustion-chamber-inlet screens with 30-percent blocking area.

(b) Original engine; combustion-chamber-inlet screens with 60- and 40-percent blocking area.

Figure 21. - Effect of combustion-chamber-inlet screens on combustion-chamber total-pressure-loss ratio for original and modified engines at altitude of 35,000 feet and flight Mach number of 0.52.

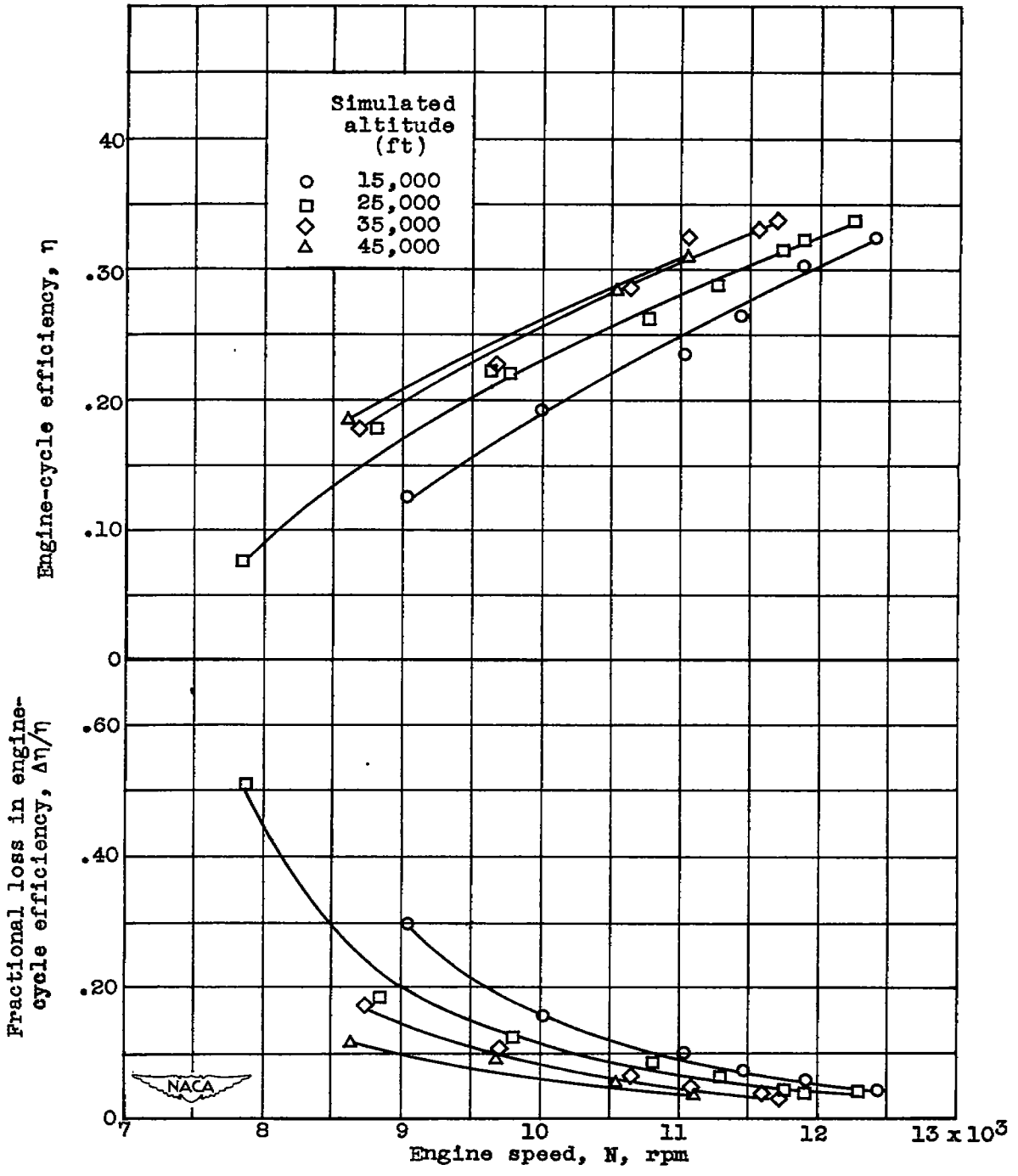

Figure 22. - Effect of engine speed and altitude on engine-cycle efficiency and fractional loss in engine-cycle efficiency for modified engine at flight Mach number of 0.52.

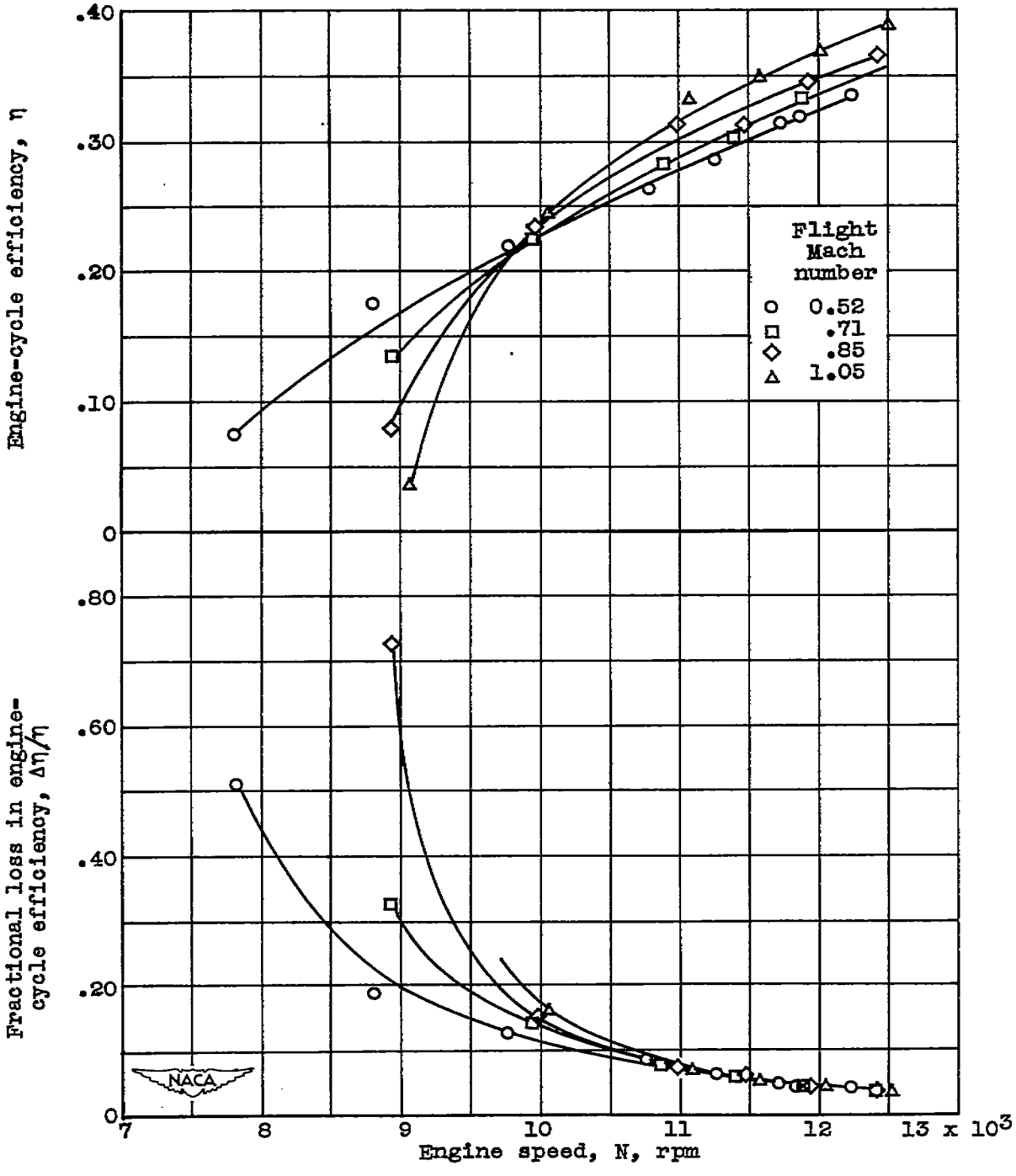

Figure 23. - Effect of engine speed and flight Mach number on engine-cycle efficiency and fractional loss in engine-cycle efficiency for modified engine at altitude of 25,000 feet.

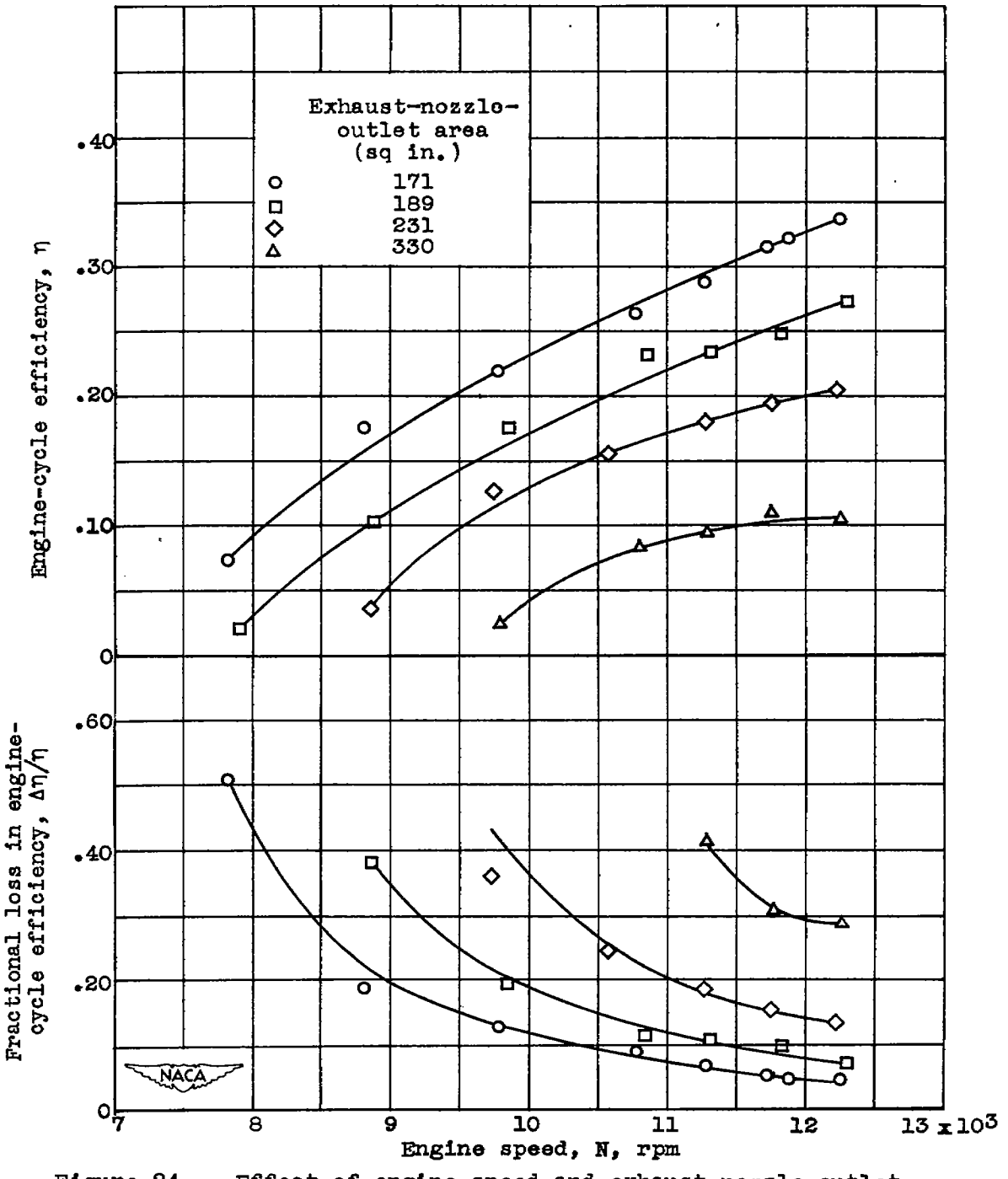

Figure 24. - Effect of engine speed and exhaust-nozzle-outlet area on engine-cycle efficiency and fractional loss in engine-cycle efficiency for modified engine at altitude of 25,000 feet and flight Mach number of 0.52.

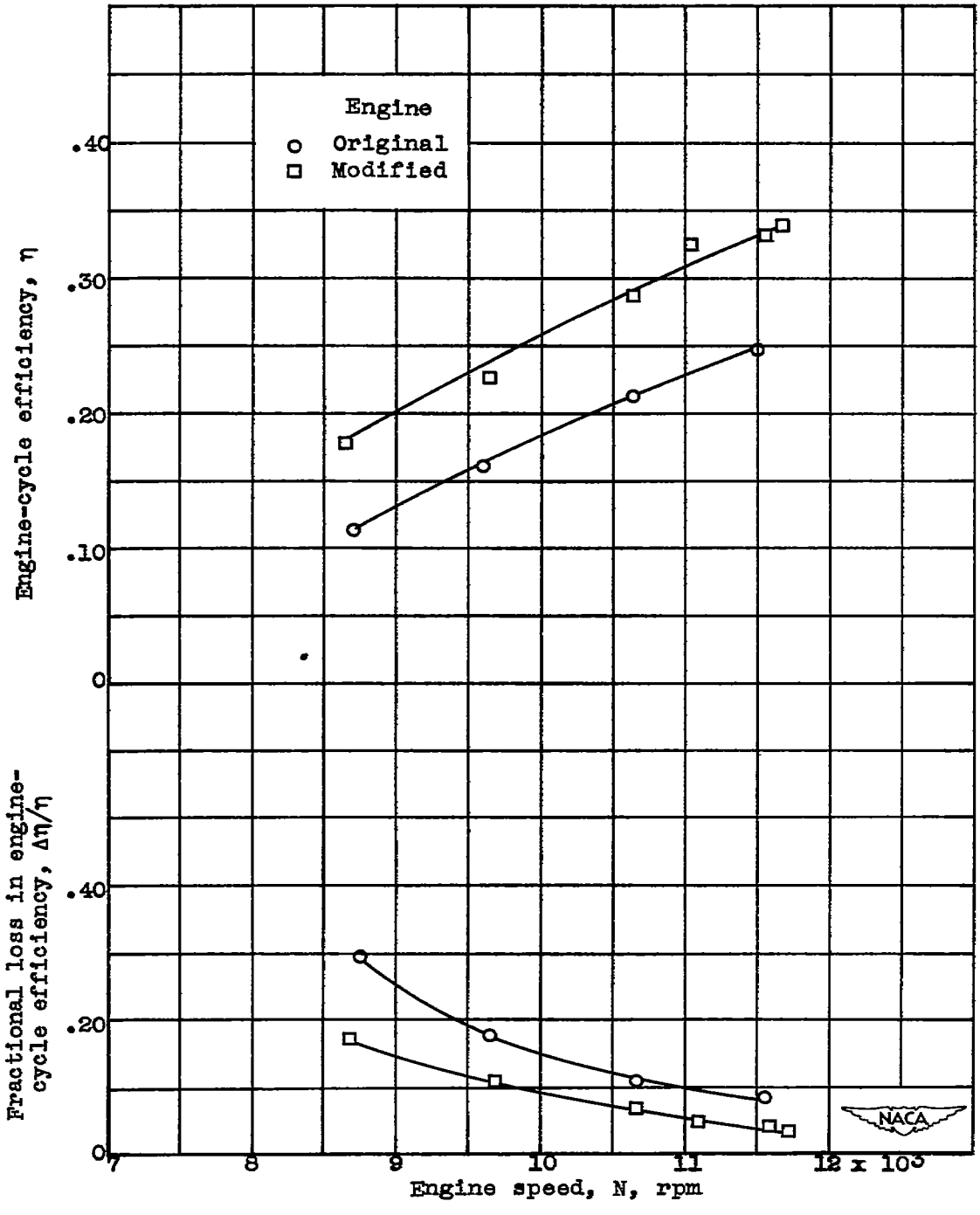

Figure 25. - Effect of engine speed on engine-cycle efficiency and fractional loss in engine-cycle efficiency for original and modified engines at altitude of 35,000 feet and flight Mach number of 0.52.

NASA Technical Library
3 1176 01435 5060